Final Report: TNT Equivalency Study for Space Shuttle (EOS)

Volume III: Appendices

Prepared by SYSTEMS PLANNING DIVISION

71 SEP 3∅

Prepared for OFFICE OF MANNED SPACE FLIGHT
NATIONAL AERONAUTICS AND SPACE ADMINISTRATION
Washington, D. C.

Contract No. NASW-2129
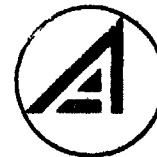
Systems Engineering Operations
THE AEROSPACE CORPORATION

FINAL REPORT: TNT EQUIVALENCY FOR SPACE SHUTTLE (EOS)

Volume III: Appendices

Prepared by

Systems Planning Division

71 SEP 30

Systems Engineering Operations
The Aerospace Corporation
El Segundo, California

Prepared for

Office of Manned Space Flight
National Aeronautics and Space Administration
Washington, D. C.

FINAL REPORT: TNT EQUIVALENCY STUDY FOR SPACE SHUTTLE (EOS)
Volume III: Appendices

Submitted by

Approved by

R. R. Wolfe, Study Manager
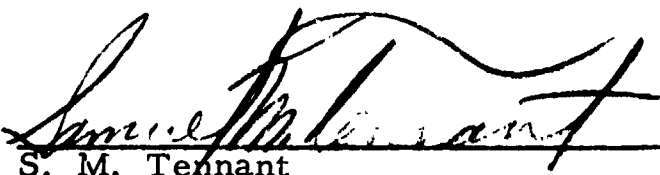
S. M. Tennant
Assistant General Manager
Systems Planning Division

PREFACE

This study was initiated as Subtask 1, TNT Equivalency Study to NASA Study C-II, Advanced Missions Safety Studies. Other studies in this series are Subtask 2, Safety Analysis of Parallel versus Series Propellant Loading of the Space Shuttle, Aerospace Report No. ATR-71(7233)-1 and Subtask 3, Orbiting Propellant Depot Safety Study, Aerospace Report No. ATR-71(7233)-3.

This study was supported by NASA Headquarters and managed by the Advanced Missions Office of the Office of Manned Space Flight. Mr. Herbert Schaefer, the Study Monitor, supported by Mr. Charles W. Childs of the NASA Safety Office, provided guidance and counsel that significantly aided this effort.

Study results are presented in three volumes; these volumes are summarized as follows:

> Volume I: Management Summary Report presents a brief, concise review of the study content and summarizes the principal conclusions and recommendations.

> Volume II: Technical Discussion provides a discussion of the available test data and the data analysis. Details of an analysis of possible vehicle static failure modes and an assessment of their explosive potentials are included. Design and procedural criteria are suggested to minimize the occurrence of an explosive failure.

> Volume III: Appendices contains supporting analyses and backup material.

PRECEDING PAGE BLANK NOT FILMED

ACKNOWLEDGEMENTS

PRECEDING PAGE BLANK NOT FILMED

CONTENTS

PRECEDING PAGE BLANK NOT FILMED

APPENDIX A

Tabulation of Pyro Test Data with
Yield in Percent TNT as Determined
by URS Systems Corp., Bellcomm Inc., and The Aerospace Corp.

In this appendix, the following table headings are defined as:

L/D_t - Tank Length/Diameter

D_o/D_t - Rupture Diaphragm Diameter/Tank Diameter

$D/W^{1/3}$ - Distance from Event/(Total Wt of Propellants)$^{1/3}$

The legend below is a key for the Ignition Source column.

A   Bottom tank did not release fluid until after impact of top tank

B   Tank rupture ignition

C   Cap ignition at tank rupture

D   Cap ignition

E   Diaphragm rupture ignition

F   Cap ignition at 100 psi internal pressure

G   Ignition caused by poor venting

H   Fire on tank before ignition

I   Squib ignition

J   Probable impact ignition

K   Fire visible at top of tank 10-15 ms before ignition

L   Ignition at impact

M   Fire at top of tank

N   Self-ignition -- suspect diaphragm break

P   Fire at top of tank after rupture, ignition at bottom of tank

Q   Tank fell through stopper

R   Fire on pad before ignition

S   Tank broke apart at impact

T   Self-ignition - tank leaked

U   Cap ignited after propellant on pad. Fire went out; detonation at time given.

Test No.	Test Config.	Prop. Wt. (lb)	L/D_t	D_o/D_t	Ignition Source†	Ignition Delay (ms)	Distance D(ft)	$D/W^{1/3}$	Avg. Pressure (psi)	Yield - % TNT Aerospace (Pressure)	URS (Terminal)	Bellcomm (Pressure)
050	CBM	200	1.8	1.0	B	180	23 37 67	3.94 6.33 11.46	31.0 16.8 6.5	80	86	79.3
093	CBM	200	1.8	1.0	D	147	23 37 67	3.94 6.33 11.46	22.0 9.0 3.5	25	34	26.1
051	CBM	200	1.8	1.0	C	80	23 37 67	3.94 6.33 11.46	12.6 7.1 3.1	17	22	16.24
0.53*	CBM	200	1.8	0.45	E	1	23 37 67	3.94 6.33 11.46	4.07 2.4 1.15	2.5	4	2.0
199	CBM	200	1.8	0.45	D	816	23 37 67 117	3.94 6.33 11.46 20.0	7.5 3.4 1.3 0.75	4	8	4.21
091	CBM	200	1.8	0.45	E	0	23 37 67	3.94 6.33 11.46	9.73 4.5 1.85	6.5	13	6.53
200	CBM	200	1.8	0.45	D	417	23 37 67 117	3.94 6.33 11.46 20.0	9.67 4.43 1.55 0.83	6	17	6.0
118	CBM	200	1.8	0.45	F	82	23 37 67	3.94 6.33 11.46	10.8 5.33 2.17	9	20	9.5
090	CBM	200	1.8	0.45	F	35 sec	23 37 67	3.94 6.33 11.46	19.4 7.8 3.25	22	29	17.5
167	CBM	133 (partial)	1.8	0.45	G	8.74 sec	23 37 67	3.94 6.33 11.46	15.55 7.8 3.4	24	24	23.94
172	CBM	133 (partial)	1.8	0.45	D,H	770	23 37 67	3.94 6.33 11.46	23.0 10.2 3.9	30	35	30.0

*Judged spurious by Bellcomm but used in URS analysis.

†Key on page A-1

Test No.	Test Config.	Prop. Wt. (lb)	L/D	D_o/D_t	Ignition Source	Ignition Delay (ms)	Distance D (ft)	$D/W^{1/3}$	Avg. Pressure (psi)	Yield - % TNT Aerospace (Pressure)	Yield - % TNT URS (Terminal)	Yield - % TNT Bellcomm (Pressure)
210	CBM	1,000	1.8	0.45	B or E	20	23 37 67 117	2.3 3.7 6.7 11.7	10.2 4.5 2.0 1.0	2	7	1.6
265	CBM	1,000	1.8	0.45	D	750	23 37 67 117 200	2.3 3.7 6.7 11.7 20.0	13.8 6.0 1.9 1.4 0.7	5	10	3.4
212	CBM	1,000	1.8	0.45	D	1366	23 37 67 117	2.3 3.7 6.7 11.7	14.0 5.2 2.8 3.3	10	27	3.2
213	CBM	1,000	1.8	0.45	E	708	23 37 67 117 200	2.3 3.7 6.7 11.7 20.0	67.2 22.7 8.1 3.2 1.6	25	35	23.3
281	CRM	25,000	1.8	0.45	E	0	600	20.5	0.1	0.05	0.1	0.05
277	CBM	25,000	1.8	0.45	E	31	67 117 200 335 600	2.3 4.0 6.85 11.5 20.5	2.9 0.9 0.5 0.12 0.1	0.05	0.2	0.09
279	CBM	25,000	1.8	0.45	E	33	335 600	11.5 20.5	0.2 0.1	0.05	0.2	0.05
057	CBM	200	5.1	1.0	F		23 37 67	3.94 6.33 11.46	2.47 1.67 0.85	1.2	1.3	1.0
052	CBM	200	5.1	1.0	I	83	23 37 67	3.94 6.33 11.46	6.87 4.25 1.75	6	7	6.1
092	CBM	200	5.1	1.0	F	3 min.	23 37 67	3.94 6.33 11.46	6.87/12 3.13/7.7 1.4/3.1	3/18	26	3.5/17.7

Test No.	Test Config.	Prop. Wt. (lb)	L/D_t	D_o/D_t	Ignition Source	Ignition Delay (ms)	Distance D (ft)	$D/W^{1/3}$	Avg. Pressure (psi)	Yield - % TNT		
										Aerospace (Pressure)	URS (Terminal)	Bellcomm (Pressure)
055*	CBM	200	5.1	0.45	B	1	23 / 37 / 67	3.94 / 6.33 / 11.46	2.6 / 1.84 / 0.95	1.5	1	1.2
054*	CBM	200	5.1	0.45	E	17	23 / 37 / 67	3.94 / 6.33 / 11.46	4.3 / 2.9 / 1.45	4	6	3.8
138	CBM	200	5.1	0.45	D	100	23 / 37 / 67	3.94 / 6.33 / 11.46	14.5 / 6.5 / 2.35	13	17	12.0
094	CBM	200	5.1	0.45	F	329	23 / 37 / 67	3.94 / 6.33 / 11.46	24.7 / 8.45 / 3.03	25	25	21.8
062	CBM	91,000 (S-IV)	2.0	0.083	Unknown	183	38 / 67 / 117 / 200 / 335 / 600	0.845 / 1.49 / 2.6 / 4.45 / 7.45 / 13.3	96.0 / 26.42 / 12.25 / 4.48 / 2.55 / 1.07	3.-	6	3.26
169	CBM	200 (Scaled S-IV)	1.8	0.083	D	318	23 / 37 / 67	3.94 / 6.33 / 11.46	12.85 / 4.9 / 2.15	9.5	15	9.0
173	CBM	200 (Scaled S-IV)	1.8	0.083	H	56	23 / 37 / 67	3.94 / 6.33 / 11.46	8.8 / 3.8 / 1.77	6	15	5.43

*Judged spurious by Bellcomm, but used in URS analysis

A-4

Test No.	Test Config.	Prop. Wt. (lb)	L/D_t	Impact Velocity (fps)	Ignition Source	Ignition Delay (ms)	Distance D(ft)	$D/W^{1/3}$	Avg. Pressure (psi)	Yield - % TNT		
										Aerospace (Pressure)	URS (Terminal)	Bellcomm (Pressure)
197	CBGS-V	200	1.8	44	D	500	23 37 67 117	3.94 6.33 11.46 20.0	16.6 7.0 2.7 1.35	15	19	16.95
230	CBGS-V	200	1.8	44	K	24	23 37 67 117 200	3.94 6.33 11.46 20.0 34.2	17.8 6.53 2.33 1.17 0.67	11-18	21	12.9
231	CBGS-V	200	1.8	44	D	525	23 37 67 117 200	3.94 6.33 11.46 20.0 34.2	18.87 8.67 2.87 1.3 0.7	20	24	16.65
203	CBGS-V	200	1.8	44	D	800	23 37 67 117	3.94 6.33 11.46 20.0 34.2	29.8 8.8 3.53 1.6	25	31	22.94
254	CBGS-V	200	1.8	44	D	533	23 37 67 117 200	3.94 6.33 11.46 20.0 34.2	17.73 8.03 3.15 1.6 0.83	30	32	24.5
252	CBGS-V	200	1.8	44	D	325	23 37 67 117 200	3.94 6.33 11.46 20.0 34.2	25.47 9.63 3.87 1.75 0.93	40	38	35.6
204	CBGS-V	200	1.8	44	D	317	23 37 67 117	3.94 6.33 11.46 20.0	26.93 11.53 4.73 1.95	40	42	44.1
229	CBGS-V	200	1.8	44	D	1,374	23 37 67 117 200	3.94 6.33 11.46 20.0 34.2	48.4 7.5 3.73 1.43 1.07	18-60	53	35.25

Test No.	Test Config.	Prop. Wt. (lb)	L/D_t	Impact Velocity (fps)	Ignition Source	Ignition Delay (ms)	Distance D(ft)	$D/W^{1/3}$	Avg. Pressure (psi)	Yield - % TNT		
										Aerospace (Pressure)	URS (Terminal)	Bellcomm (Pressure)
251	CBGS-V	200	1.8	44	D	775	23 37 67 117 200	3.94 6.33 11.46 20.0 34.2	39.6 11.9 4.15 2.05 1.13	30-60	64	51.2
211	CBGS-V	1,000	1.8	44	L	0	23 37 67 117	2.3 3.7 6.7 11.7	26.3 8.7 3.6 1.9	5	12	4.94
266	CBGS-V	1,000	1.8	44	M	0	23 37 67 117 200	2.3 3.7 6.7 11.7 20.0	31.8 12.4 4.0 1.83 0.9	8	14	6.76
264	CBGS-V	1,000	1.8	44	N	21	23 37 67 117 200	2.3 3.7 6.7 11.7 20.0	44.9 16.3 5.05 2.5 1.3	15	22	11.36
217	CBGS-V	1,000	1.8	44	D	1,490	23 37 67 117 200	2.3 3.7 6.7 11.7 20.0	112.8 23.6 6.7 2.3 1.6	25	33	28.2
262	CBGS-V	1,000	1.8	44	D	900	23 37 67 117 200	2.3 3.7 6.7 11.7 20.0	101.6 26.1 10.1 4.2 1.9	40	42	36.9
289	CBGS-V	25,000	1.8	44	Unknown	166	67 117 200 335 600	2.29 4.0 6.84 11.5 20.5	15.0 6.23 2.47 1.2 0.6	3	4	2.7
290	CBGS-V	25,000	1.8	44	P	105	67 117 200 335 600	2.29 4.0 6.84 11.5 20.5	14.0 5.77 2.4 1.13 0.5	3	4	2.15

Test No.	Test Config.	Prop. Wt. (lb)	L/D_t	Impact Velocity (fps)	Ignition Source	Ignition Delay (ms)	Distance D(ft)	$D/W^{1/3}$	Avg. Pressure (psi)	Yield - % TNT		
										Aerospace (Pressure)	URS (Terminal)	Bellcomm (Pressure)
288C	CBGS-V	25,000	1.8	44	Unknown	365	67 117 200 335 600	2.29 4.0 6.84 11.5 20.5	38.0 17.0 5.8 2.2 1.07	10-15	13	10.2
150	CBGS-V	200	1.8	78	D	40	23 37 67	3.94 6.33 11.46	26.93 9.67 4.03	25-30	35	34.2
151	CBGS-V	200	1.8	78	D, Q	167	23 37 67	3.94 6.33 11.46	23.93 11.63 4.5	40	46	35.2
226*	CBGS-V	200	1.8	78	R	283	23 37 67 117 200	3.94 6.33 11.46 20.0 34.2	33.35 7.97 4.03 1.8 1.03	50	51	37.0
114	CBGS-V	200	1.8	76	D	74	23 37 67	3.94 6.33 11.46	29.5 15.4 5.43	60	54	52.0
195	CBGS-V	200	1.8	78	D	292	23 37 67 117	3.94 6.33 11.46 20.0	48.97 12.77 5.43 3.05	100	104	53.6
216	CBGS-V	1,000	1.8	78	L	0	23 37 67 117 200	2.3 3.7 6.7 11.7 20.0	27.6 9.4 3.7 1.63 0.8	6	9	5.5
215	CBGS-V	1,000	1.8	78	S	20	23 37 67 117 200	2.3 3.7 6.7 11.7 20.0	53.4 15.9 5.3 2.4 1.23	15	20	12.13

*Judged spurious by Bellcomm, but used in URS analysis

Test No.	Test Config.	Prop. Wt. (lb)	L/D_t	Impact Velocity (fps)	Ignition Source	Ignition Delay (ms)	Distance D(ft)	$D/W^{1/3}$	Avg. Pressure (psi)	Yield - % TNT Aerospace (Pressure)	URS (Terminal)	Bellcomm (Pressure)
105	CBGS-V	200	1.8	23	D	0	23 37 67	3.94 6.33 11.46	9.63 4.15 1.75	6	7	6.04
152	CBGS-V	200	1.8	23	D	480	23 37 67	3.94 6.33 11.46	13.57 5.84 2.53	11	14	11.9
153	CPGS-V	200	1.8	23	D	121	23 37 67	3.94 6.33 11.46	15.5 6.57 2.5	13	14*	12.8
184	CBGS-V	200	1.8	23	D	810	23 37 67	3.94 6.33 11.46	14.9 7.1 2.87	16	17	16.3
201	CBGS-V	200	1.8	23	D	1,524	23 37 67 117	3.94 6.33 11.46 20.0	29.9 10.4 3.4 1.4	20-30	26	26.0
225	CBGS-V	200	1.8	23	D	933	23 37 67 117 200	3.94 6.33 11.46 20.0 34.2	14.03 6.43 3.07 1.5 0.9	11-30	34	23.9
113	CBGS-V	200*	5.0	78	D	77	23 37 67	3.94 6.33 11.46	38.77 14.13 4.93	45	52	
115	CBGS-V	200*	5.0	78	D	93	23 37 67	3.94 6.33 11.46	10.0 4.87 2.17	9	15	
164	CBGS-V	200	5.0	23	T	125	23 37 67	3.94 6.33 11.46	6.1 2.67 1.4	3.5	4	
104	CBGS-V	200	5.0	23	I	258	23 37 67	3.94 6.33 11.46	9.2 4.07 1.7	5.5	6	

*Propellants reversed (LO$_2$ on top)

Test No.	Test Config.	Prop. Wt. (lb)	L/D_t	Impact Velocity (fps)	Ignition Source	Ignition Delay (ms)	Distance D(ft)	$D/W^{1/3}$	Avg. Pressure (psi)	Yield - % TNt		
										Aerospace (Pressure)	URS (Terminal)	Bellcomm (Pressure)
165	CBGS-V	200	5.0	23	U	325	23 37 67	3.94 6.33 11.46	10.85 4.53 2.07	8	8	
103A	CBGS-V	200*	5.0	23	D	208	23 37 67	3.94 6.33 11.46	21.8 10.87 3.9	26.5	39	
161	CBGS-V	200	5.0	78	D	0	23 37 67	3.94 6.33 11.46	8.75 3.9 1.67	5	5	
116	CBGS-V	200	5.0	78	L	18	23 37 67	3.94 6.33 11.46	10.63 5.2 2.13	9	10	
160	CBGS-V	200	5.0	78	D	67	23 37 67	3.94 6.33 11.46	24.8 9.6 4.13	25-30	32	

*Propellants reversed (LO_2 on top)

A-9

Test No.	Test Config.	Prop. Wt. (lb)	L/D_t	Impact Velocity (fps) Lower	Impact Velocity (fps) Upper	Ignition Source	Ignition Delay (ms)	Distance D (ft)	$D/W^{1/3}$	Avg. Pressure (psi)	Yield - % TNT Aerospace (Pressure)	Yield - % TNT URS (Terminal)	Yield - % TNT Bellcomm (Terminal)
183	CBGS-H	200	1.8	12	78	J	0	23 37 67	3.94 6.33 11.46	17.3 6.75 2.6	15	15	
196	CBGS-H	200	1.8	12	78	D	77	23 37 67 117	3.94 6.33 11.46 20.0	17.13 6.43 2.37 1.2	15	17	
228	CBGS-H	200	1.8	12	78	Unknown	42	23 37 67 117 200	3.94 6.33 11.46 20.0 34.2	25.63 9.1 3.73 1.77 0.87	30	34	
253	CBGS-H	200	1.8	12	78	D	108	23 37 67 117 200	3.94 6.33 11.46 20.0 34.2	26.33 11.3 4.2 1.55 1.07	35	57	
132	CBGS-H	200	1.8	12	23	D, A	0	23 37 67	3.94 6.33 11.46	8.27 3.43 1.53	4.5	5	
133A	CBGS-H	200	1.8	12	23	D	286	23 37 67	3.94 6.33 11.46	9.0 3.83 1.5	5	6	
185	CBGS-H	200	1.8	12	23	J	0	23 37 67	3.94 6.33 11.46	8.6 4.05 1.77	6	8	
186	CBGS-H	200	1.8	12	23	Unknown	61	23 37 67	3.94 6.33 11.46	10.83 4.77 2.13	9	9	
224	CBGS-H	200	1.8	12	23	D	899	23 37 67 117 200	3.94 6.33 11.46 20.0 34.2	13.97 6.07 2.6 1.25 0.57	13	16	
223	CBGS-H	200	1.8	12	23	D	157	23 37 67 117 200	3.94 6.33 11.46 20.0 34.2	14.1 5.5 2.43 1.3 0.65	17	18	

APPENDIX B

Summary of Test Methods Employed by Investigators

CONTENTS

FIGURES

B. 1   GENERAL

The data produced by these tests are summarized and analyzed in Volume II. The purpose of this appendix is to present the configurations and pertinent parameters used in the test programs.

B. 2   A. D. LITTLE, INC., SPILL TESTS (Ref. B-1)

A. D. Little, Inc. conducted a series of LO_2/LH_2 spill tests in 1962. All tests were conducted with an oxidizer-to-fuel ratio of 5 to 1. Nine tests involved a total propellant weight of 45 lb each, and three of 225 lb each.

As shown in Figure B-1, tanks containing the LO_2 and LH_2 were tipped toward each other, spilling the propellants in partially impinging streams into a shallow pit to achieve active mixing. Tank release was sequenced to ensure that both tanks were exhausted simultaneously. An explosive charge in the spill pit was used to initiate the explosion in all tests.

Overpressure was sensed by piezoelectric pressure transducers, and was recorded by photographing an oscillograph trace. Five gauges were positioned along a single radial line from the explosion. Distances varied from 30 to 70 ft in the 45-lb tests, and from 60 to 120 ft in the 225-lb tests.

Test results were reported in terms of pressure yield, calculated by averaging the pressure yields determined individually for each data point. The TNT reference curve used in determining yield was developed experimentally by A. D. Little, since their test program preceded the publication of the currently accepted TNT curves prepared by Ballistic Research Labs. (BRL) (Ref. B-2).

B. 3   NASA SPILL AND TANK TESTS (Ref. B-3)

In 1964, NASA-MFSC conducted a series of LO_2/LH_2 tests. Each of these tests involved 200 lb of propellants, and an oxidizer-to-fuel ratio of 5 to 1. Six spill tests and seven tank tests were run.

PRIMACORD

LH₂

PRIMACORD

EXPLOSIVE
CHARGE

LOX
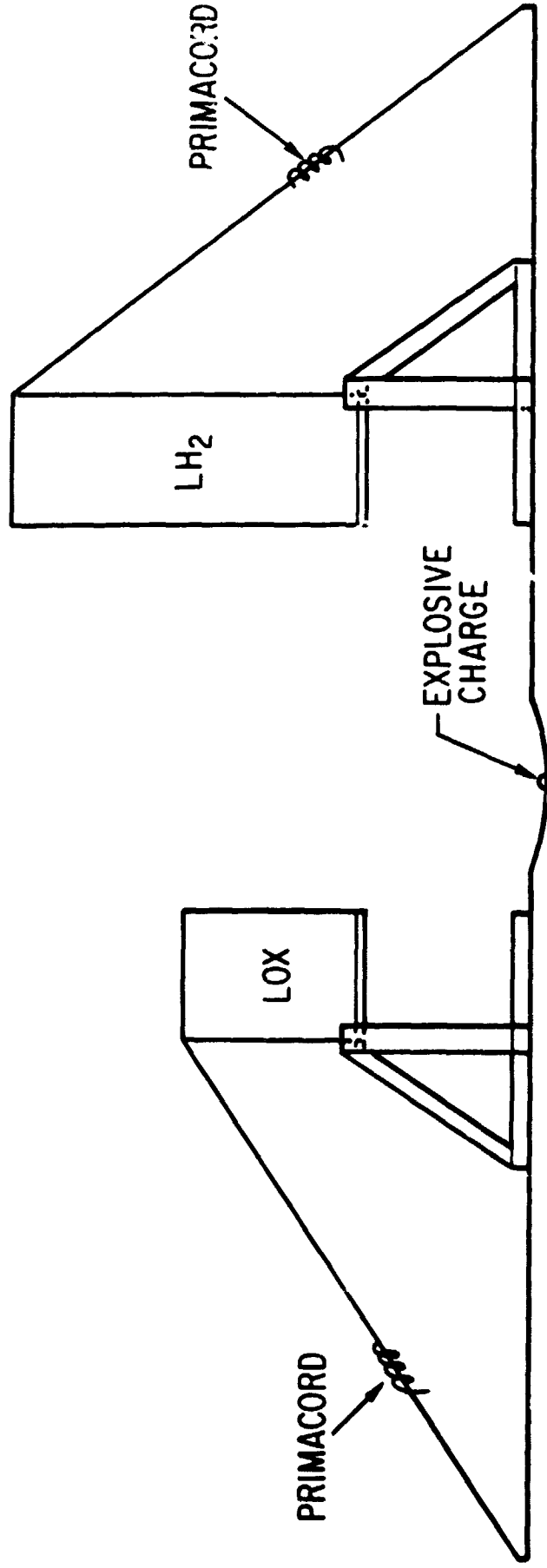
- $LO_2 - LH_2$ wt. ratio 5:1
- Aluminum containers
- Propellants spilled simultaneously in partially impinging streams
- A. D. Little – 9 tests at 45 lb and 3 tests at 225 lb total propellant wt.
- NASA tests all 200 lb total propellant wt. (6 tests)

Figure B-1. Spill Test Programs (A. D. Little and NASA-MFSC)

The description of the test method employed in the A. D. Little spill test is applicable also to the NASA spill test method (Figure B-1). In the tank tests, the propellants were contained in tandem tanks, separated by an intertank bulkhead (Figure B-2). The simulated failure modes included intertank bulkhead rupture and tank wall rupture. Bulkhead rupture was produced either by overpressurization or by detonating a linear-shaped charge attached to the structure. Tank wall rupture was accomplished by a linear-shaped charge.

It was intended to control ignition delay by utilizing either a squib (for flame ignition) or a blasting cap (for shock ignition). However, in all tests ignition was spontaneous at tank failure and was probably caused by the shock accompanying the tank failure.

Overpressure was sensed by piezoelectric pressure transducers and recorded on magnetic tape. Six gauges were positioned along a radial line at distances ranging from 25 to 250 ft. Three additional gauges were located in a radial line 45 deg away from the first line, and at distances of 25 to 65 ft from the test article. Four gauges were spaced along a third radial line, 80 deg away from the first line, at distances of 25 to 100 ft.

For each series of tests a range of pressure and impulse yields was reported. The ranges were determined by plotting the high and low TNT yield percentage curves which envelop all of the data points. The BRL-TNT curves were used as the reference basis. No tabulated test data were reported.

B. 4   AEROJET-GENERAL CORP. CONTROLLED INTERFACE TESTS (Ref. B-4)

In 1965, AGC conducted a series of LO_2/LH_2 tests to evaluate the explosive characteristics of these propellants. The propellants were combined using a mixing technique that permitted controlled variation of the oxidizer/fuel contact area and the weight of propellant. A fixed 5 to 1 oxidizer-to-fuel ratio was used for all of these tests. The propellants were mixed by placing oxidizer-filled glass dewars in a fuel-filled pan and shattering the dewars

FLSC

FLSC

LH₂

LOX

INTERNAL
FLSC

LH₂

LOX

EXTERNAL
FLEXIBLE LINEAR
SHAPED CHARGE
(FLSC)

LH₂

LOX

DIAPHRAGM

C-4 EXPLOSIVE
CHARGE

LH₂

LOX
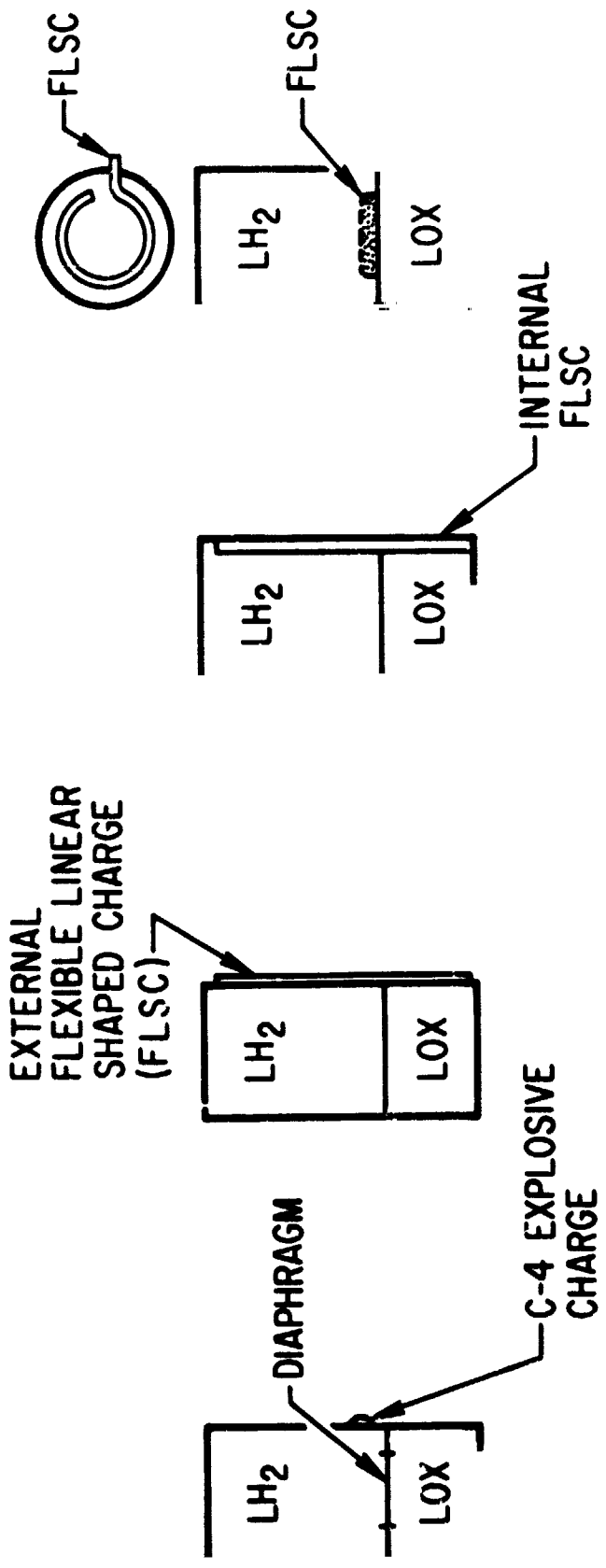
- Propellants separated by intertank bulkhead

- Simulated failure modes - intertank bulkhead rupture and tank split

- Total of 7 tests, each with 200 lb total propellant wt.

- $LO_2 - LH_2$ wt. ratio - 5:1

Figure B-2. NASA-MSFC Tank Failure Test Program

with an explosively generated shockwave (Figure B-3). Two tests were run at each of three weights: 100, 150, and 225 lb. A constant 4 to 1 ratio of contact area between the oxidizer and fuel (in ft^2) to total propellant weight (in lb) was maintained for all tests.

Overpressure was sensed by piezoelectric transducers and recorded on magnetic tape. Four gauges were positioned along each of three radial lines spaced 120 deg apart. Gauge distances from the test article varied from 25 to 98 ft.

Test results were reported in terms of pressure yield. Yield was determined by superimposing the test data points on plots of TNT percentage yields. The TNT reference curves were determined experimentally and were reported as being in good agreement with the BRL curves. Tabulated test data were reported.

B.5   URS SYSTEMS CORP. PROJECT PYRO TESTS (Ref. B-5)

Project Pyro, conducted in the 1965-1967 time period, had as its objective the development of a reliable philosophy for predicting the credible damage potential which may be experienced from the accidental explosion of liquid propellants. Two general failure modes were simulated. In the Confinement by Missile mode (CBM) failure occurs in the intertank bulkhead, and all propellant mixing occurs within the tanks. The Confinement by Ground Surface (CBGS) condition simulated the case where the propellants spill from the tanks and mix on the ground surface. Both vertical (CBGS-V) and horizontal (CBGS-H) spill cases were simulated. A total of 78 tests were conducted and raw data were reported; 28 were in the CBM mode, 39 were CBGS-V and 11 were CBGS-H. The variations in test article parameters and configurations for the three modes, as well as the general arrangements of the test setups, are depicted in Figures B-4, B-5, and B-6.

Overpressure sensing was accomplished with piezoelectric transducers, and data were recorded on magnetic tape. Three radial lines of gauges were used,
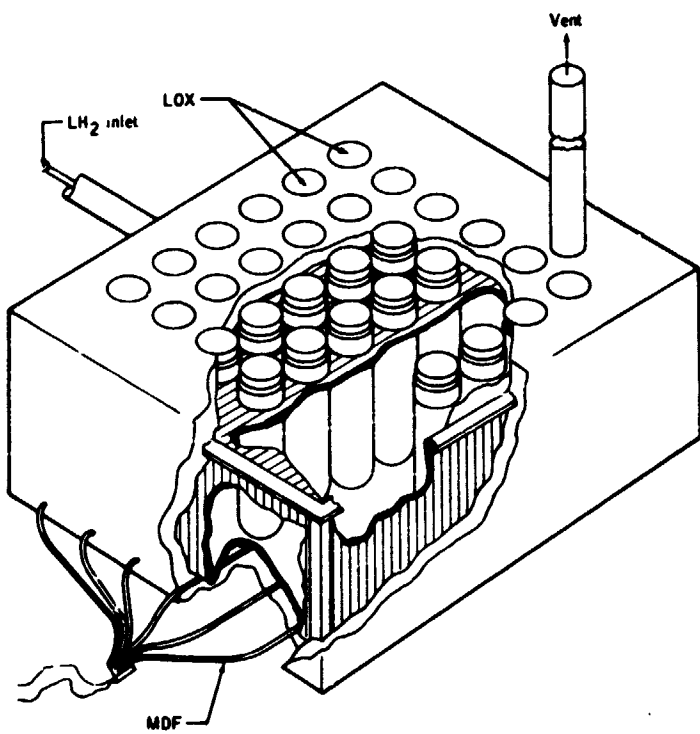
- LH$_2$ in Aluminum Container

- LO$_2$ in 1 Liter Glass Dewars

- Oxidizer/Fuel Weight Ratio 5:1 (Constant)

- 0.25 ft^2 Contact Area per Pound of Propellant (Constant)

- Dewars Shattered by Mild Detonating Fuse Under the Container Bottom

No. of Tests	Total Propellant Wt. (lb)	Container Size (in.)	No. of Dewars	Contact Area (ft^2)
2	100	12 × 24 × 24	36	25.1
2	150	12 × 34 × 36	52	36.8
2	225	12 × 44 × 44	81	56.2

Figure B-3. Aerojet-General Corporation Test Program

spaced 120 deg apart. Five transducers were positioned along each line. Distances varied from 23 to 67 ft for the 200 and 1,000-lb tests, and from 38 to 600 ft for the 25,000 and 91,000-lb tests.

Test results were reported as terminal yield, which was apparently an average of the pressure and positive phase impulse yields. The BRL-TNT pressure and impulse curves were used as a reference. Tabulated data for each test were reported.
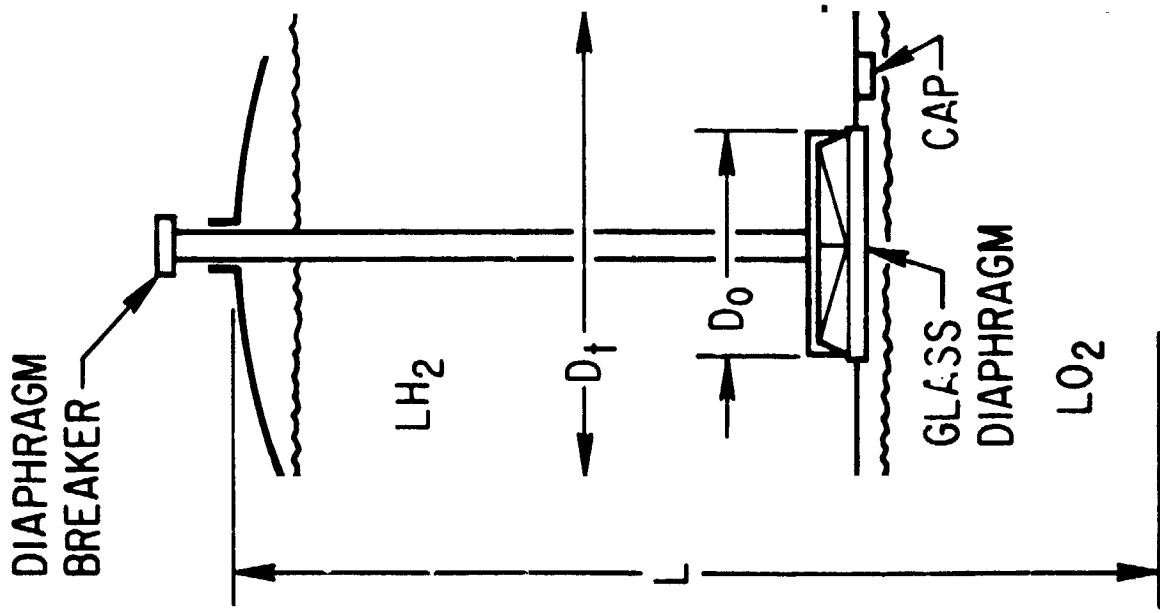
- Propellants separated by glass diaphragm

- LH_2 tank pressurized to 30 psi

- Glass diaphragm shattered by mechanical breaker

- Planned ignition by squib or blasting cap

- LO_2/LH_2 wt. ratio 5:1

- Parameters varied:
  - Total propellant wt. (200, 1000, and 25,000 lb)
  - L/D_t ratio - 1.8:1 and 5:1
  - D_o/D_t ratio - 0.083, 0.45, and 1.0:1

- Single full-scale Saturn S-IV test conducted
  - 91,000 lb LO_2-LH_2
  - L/D_t ratio 2.0, D_o/D_t ratio 0.083:1
  - S-IV aluminum intertank bulkhead ruptured by mechanical breaker

DIAPHRAGM BREAKER

LH_2

D_t

D_o

CAP

GLASS DIAPHRAGM

LO_2

Figure B-4. Project Pyro Test Program, Confined by Missile
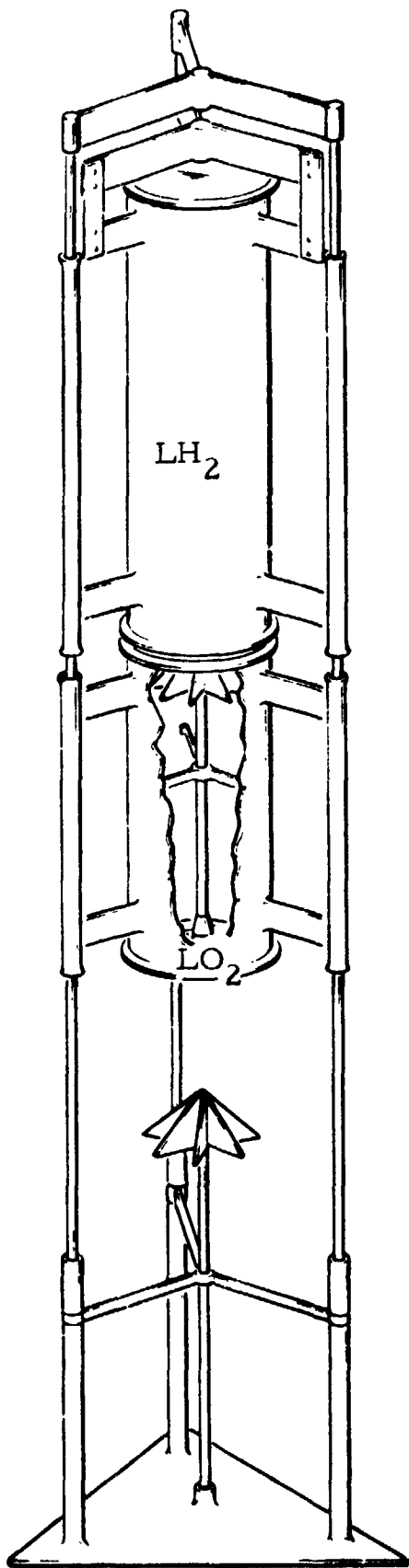
- Tandem tanks with 5 mil aluminum foil bottoms

- Tanks dropped to within 1-1/2 tank diameters of pad

- Tank bottoms ruptured simultaneously by star cutters

- Propellants spill onto pad, forming overlapping pools

- Planned ignition by linear charge

- LO_2 / LH_2 weight ratio 5:1

- Parameters varied:

  - Total propellant wt. (200, 1000, and 25,000 lb)

  - L/D ratio (1.8 and 5.0:1)

  - Impact velocity (23, 44, and 78 fps)

Figure B-5. Project Pyro Test Program, Confined by Ground Surface-Vertical
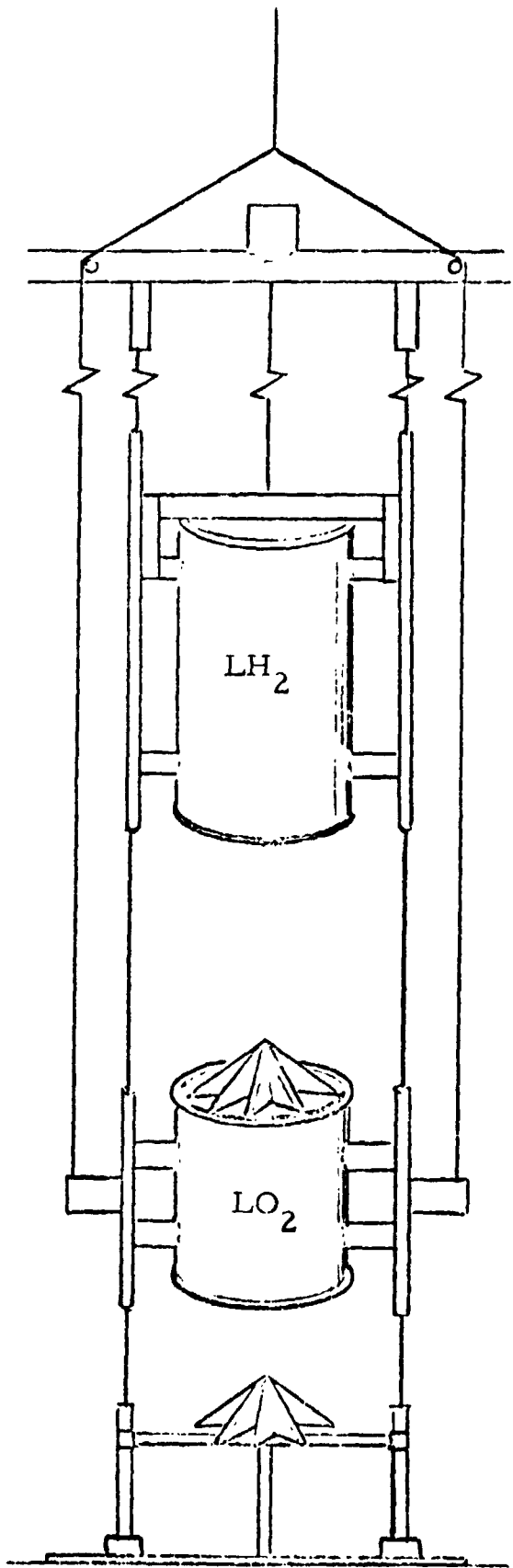
- Separate tanks with aluminum foil bottoms

- Tanks dropped separately - bottom tank stopped within 1-1/2 diameters of pad

- Tank bottoms ruptured by star cutters

- Propellants spill onto pad, forming overlapping pools

- Planned ignition by linear charge

- LO_2 / LH_2 weight ratio - 5:1

- All tests 200 lb total propellant weight

- LO_2 tank impact velocity 12 fps (all tests)

- LH_2 tank impact velocities 23 fps and 78 fps

- L/D ratio 1.8:1 (all tests)

Figure B-6.   Project Pyro Test Program, Confined by Ground Surface-Horizontal

APPENDIX B REFERENCES

B-1   "Summary Report on a Study of the Blast Effect of the Saturn Vehicle,"
       Arthur D. Little, Inc. (15 February 1962).

B-2   C. N. Kingery and B. F. Pennill, "Peak Overpressure vs Sealed
       Distance for TNT Surface Bursts," Ballistic Research Laboratories
       Memorandum Report No. 1518 (April 1964).

B-3   J. B. Gayle, et al., "Preliminary Investigation of Blast Hazards of
       RP1/LOX and LH_2/LOX Propellant Combinations," NASA, George
       Marshall Space Flight Center (9 April 1965).

B-4   R. E. Pesante and M. Nishibazashi, "Evaluation of the Blast Param-
       eters and Fireball Characteristics of Liquid Oxygen/Liquid Hydrogen
       Propellant," Aerojet-General Corp. (7 April 1967).

B-5   A. B. Willoughby, C. Wilton, and J. Mansfield, "Liquid Propellant
       Explosive Hazards," URS Systems Corp. Report URS-652-35, Vol. 1,
       2, and 3 (December 1968).

APPENDIX C

Overview of Analytical Studies Conducted at the
University of Florida

CONTENTS

FIGURES

TABLE

C. 1 GENERAL

This appendix contains a brief synopsis of studies conducted at the University of Florida under the direction of Dr. E. A. Farber.

The studies to be discussed are: the construction of a mathematical model for predicting explosive yields of liquid propellants, a seven chart approach for systematically applying the model, and the critical mass phenomena. These studies are thoroughly documented in Refs. C-1 through C-5.

C. 2 MATHEMATICAL MODEL

The mathematical model begins with the assumption that the explosive yield function is related to a mixing function where the yield function, y, is defined as a fraction of maximum theoretical yield, and the mixing function, x, is defined as the fraction of propellants actually mixed. By dealing with the yield function and the mixing function in this way, a generalized expression can be developed which is assumed to be applicable to all liquid propellants.

Using test data produced by A. D. Little (Ref. C-6), Figure C-1 was constructed and a least squares fit of the data points shown. Data points J1, J2, J3, are from tests made with a 1/25th scale Saturn V vehicle, while data points D and H were maximum values observed in smaller scale testing of a Saturn V configuration. In each case, the quantity of propellants mixed at the time of ignition was known so that the fraction of propellants mixed could be plotted against the fraction of the theoretical yield that was observed. The plot of the data suggests a relationship between the fraction of theoretical yield and the fraction of propellants mixed of the form $y = C(x)^d$, where $0 \le x \le 1$, $0 \le y \le k$, and $k < 1$. The yield function and the mixing function each are presumed to be a random variable.
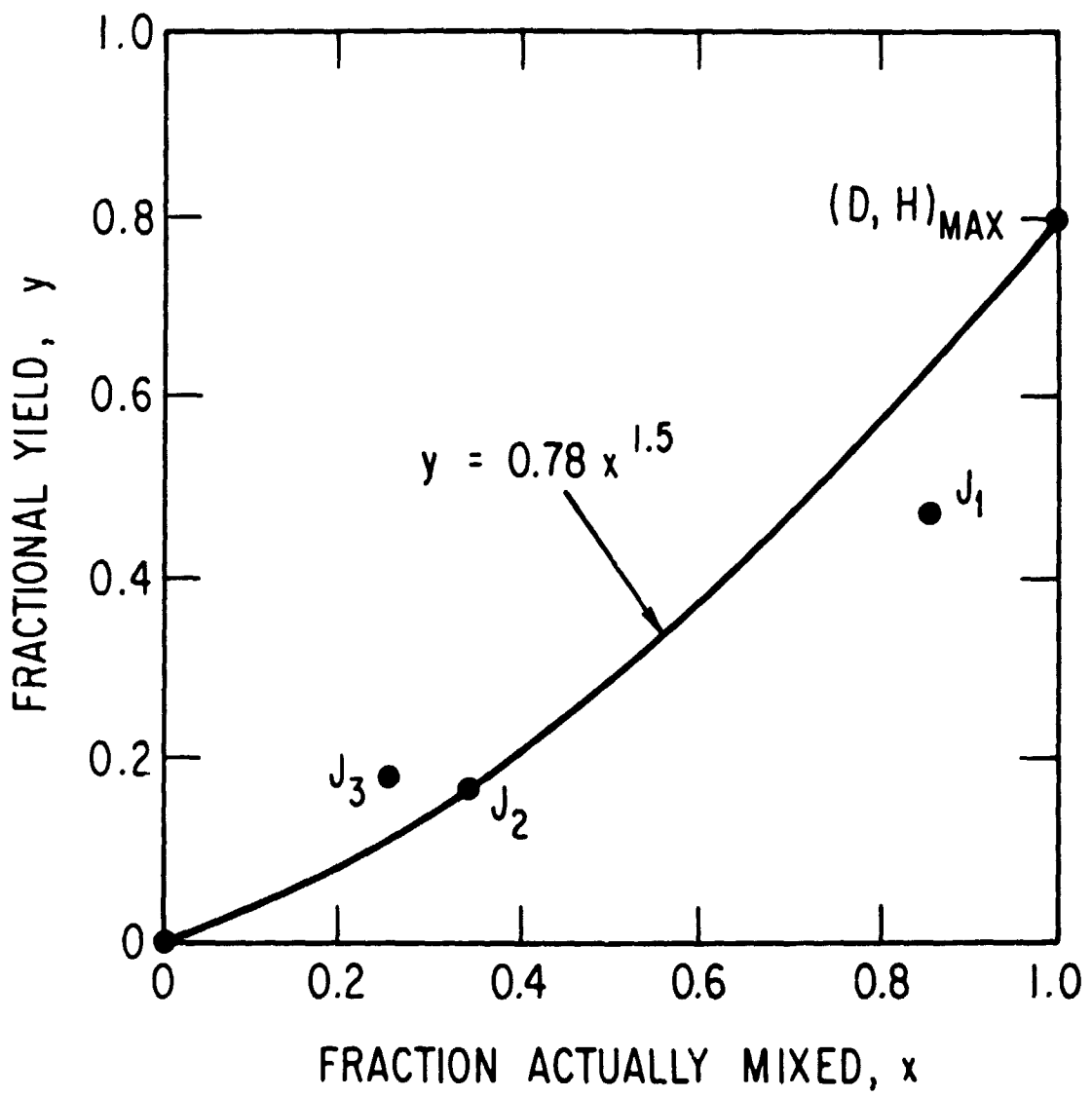
Figure C-1.   Fractional Yield vs Fraction Mixed Liquid Propellants

Moving forward with the assumption that the mathematical model does represent a generalized statement of explosive yield, a mathematical problem was addressed to find a bi-variant probability density function where the expected mean value of the yield for any given mixing function value is:

$$E(x, y) = C_x^d$$

$$= \int_0^1 \frac{f(x, y)}{\left[\int_0^{x^d} f(x, y)dy\right]} y$$

The following bi-variant function was selected for x and y.

$$f(x, y) = \frac{d\tau(a + b + c)}{\tau(a)\tau(b)\tau(c)} x^{d-1}(1 - x^d)^{a-1} y^{b-1}(x^d - y)^{c-1}$$

The only restrictions on this equation are given as $y > 0$, $x > 0$, $y \leq x^d$, and $d \neq 0$.

Mathematical relations were defined which permitted estimating the values of parameters a, b, c and d using experimental explosion data. It was determined that three of these four controlling parameters are constants: $b = 4.0$, $c = 1.1$, $d = 1.5$. Parameter a is variable and it was demonstrated that it varies with the propellant weight and is thus a scaling function applicable to the model.

When the controlling parameters of the probability distribution have been estimated, it is possible to determine the probability distribution for the yield function, the probability distribution for the mixing function, the combined yield-mixing probability distribution, and confidence limits for the yield function, and the mixing function can be assigned. The typical shape of the mathematical model represented by a statistical surface is illustrated in Figure C-2 and is likened to a shark fin.

C-3

Figure C-2. Statistical Surface of Explosive Yield Model

The relationships of the scaling factor, parameter a, to propellant weight
and to explosive yield are shown in Figure C-3. The smaller the value of
parameter a, the higher the yield, and, based on existing data points, higher
propellant weights are associated with smaller values of parameter a. It
must be emphasized that these two relationships have been developed using
experimental explosion and accidental missile failure data in order to estimate
the value of parameter a. The model is so completely flexible that other values
of parameter a could derive from different experimental or missile failure data.
Different values of a could substantially change predicted yields. The greater
the size of the data bank, the greater the confidence that may be associated
with yield predictions from this mathematical model.

A plot of explosive yield as a fraction of the potential yield versus propellant
weight is shown in Figure C-4; also the 95% probability limit is indicated.
Superimposed are data plotted from Project Pyro and from a number of actual
missile failures shown in Table C-1, where the explosive yield has usually been
estimated on the basis of analysis of resulting damage. It can be said that
the available data fit well within the prediction limits presented. It is also
evident that the fit is obtained because these data were used to determine the
controlling parameters of the prediction equation. Again, the lack of data
points above approximately 250, 000 lb of propellants gives rise to some doubt
as to the propriety of extrapolating to propellant weights in the millions of
pounds range.

C.3   SEVEN CHART APPROACH

A systematic procedure for the analytical prediction of the yield from liquid
propellants was also developed. The procedure is summarized in seven charts
(Refs. C-1, C-4, and C-5). This method has the potential to produce more
information concerning explosions and their yield, but it also requires
considerably more input information and knowledge about the liquid propellants
and the mechanisms contributing to the explosion. The input information is
not presently available in many cases and therefore was assumed in developing
the theory.
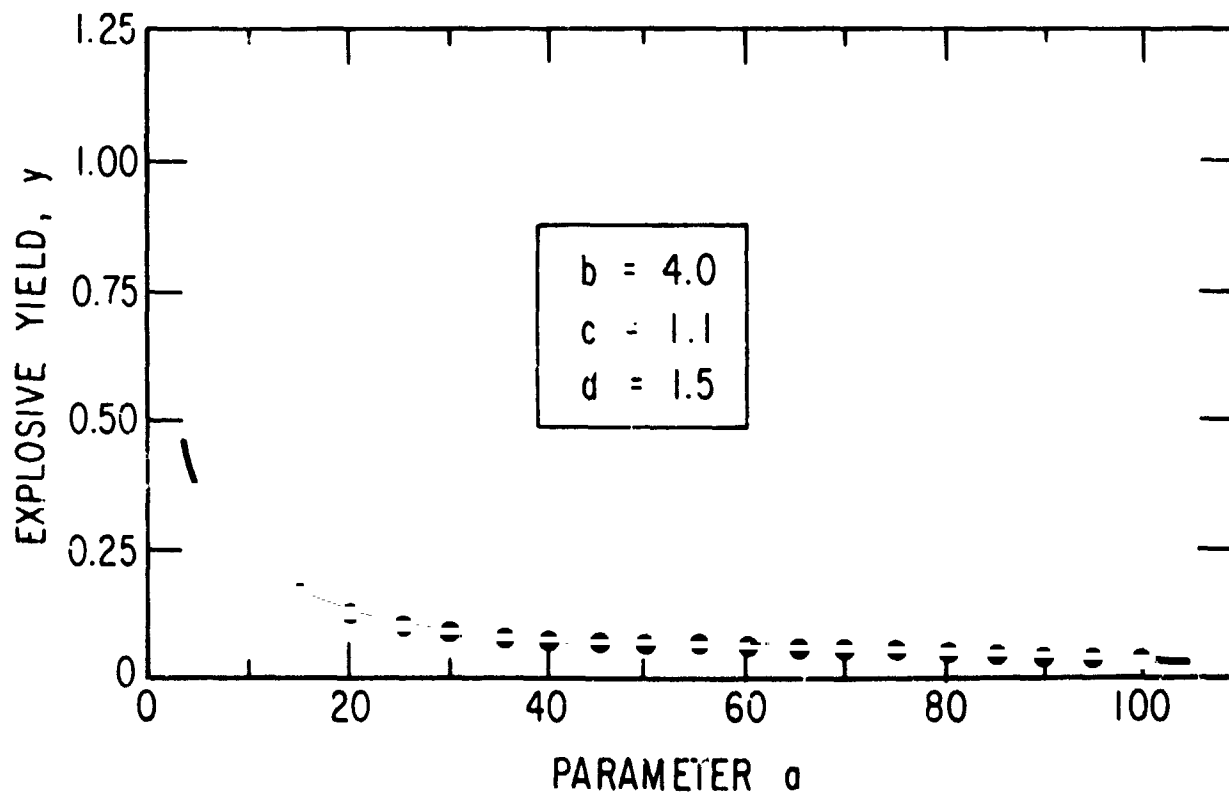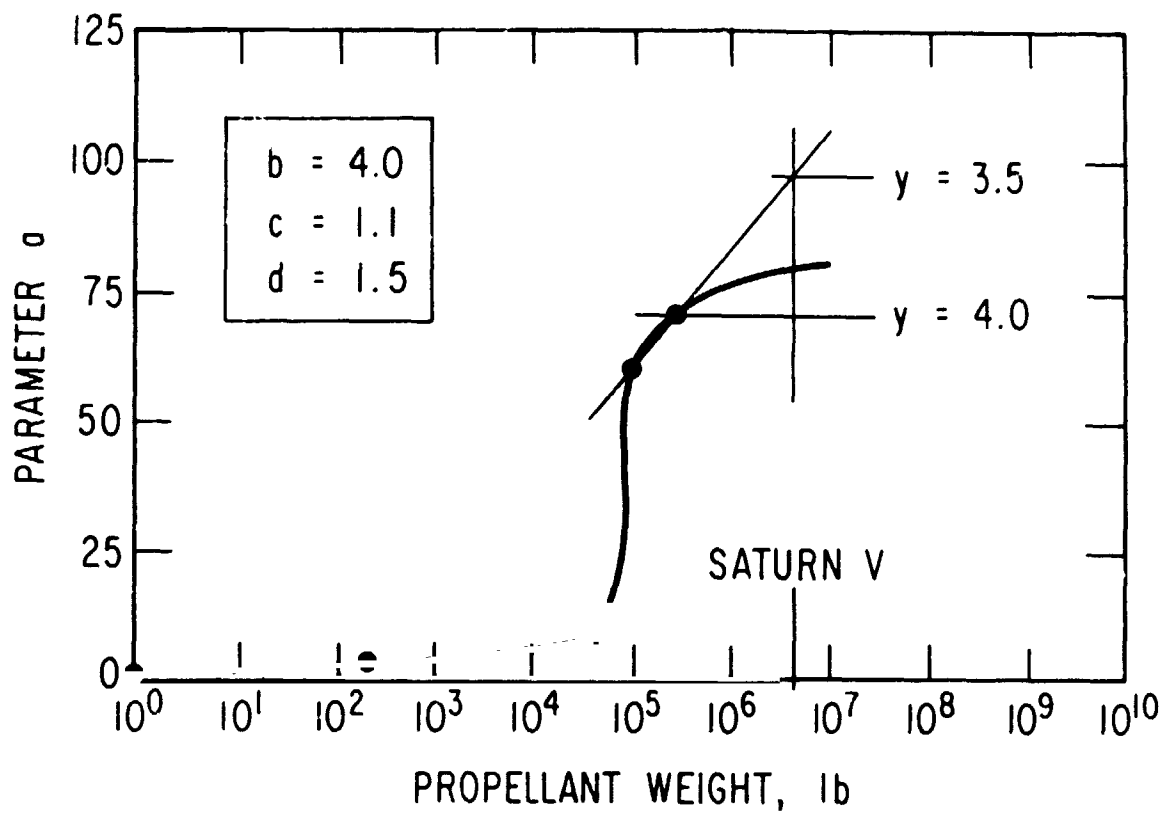
Figure C-3. Relationships of Scaling Parameter a to Propellant Weight and to Explosive Yield
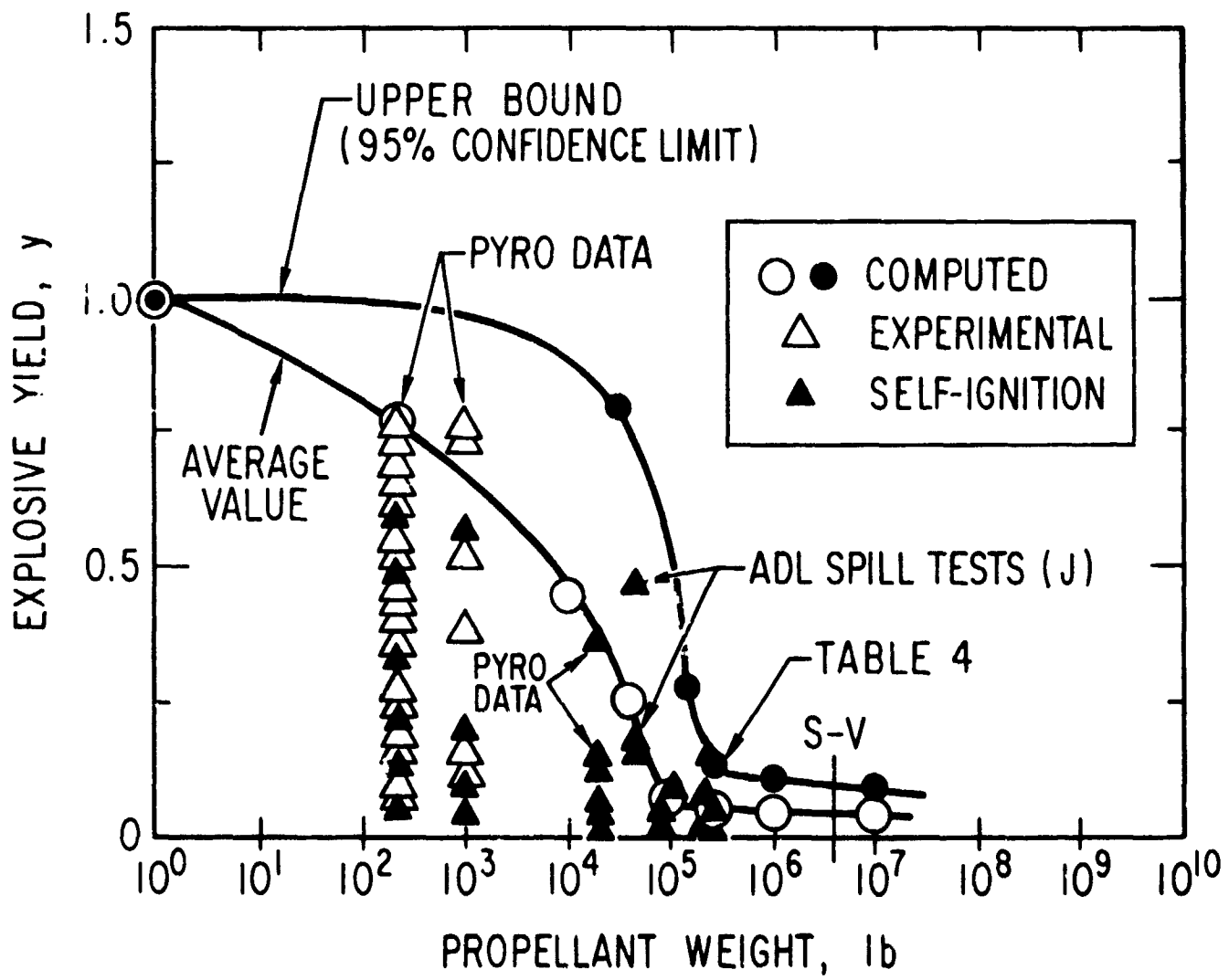
Figure C-4. Estimated Explosive Yield vs Propellant Weight, Liquid Propellants

Table C-1. Yield Estimates and Data of Missile Failures

		Weight(k lb)	Yield, TNT	Yield, Norm.
Atlas 9-C	LOX/RF	250	0.18	0.147
Atlas 48-D	LOX/RP	250	0.08	0.065
Atlas	LOX/RP	250	0.06	0.049
Titan 1 (Impact)	Hyp.	230	0.02	0.016
Titan 1	Hyp.	230	0.01	0.008
Atlas	LOX/RP	250	0.0088	0.008
Centaur	LOX/RP/LH$_2$	282	0.029	0.024
Jupiter 9 (Impact)*	LOX/RP	120	0.11	0.09
S-IV Failure	LOX/LH$_2$	100	0.01	0.008
S-IV Test (Pyro)	LOX/LH$_2$	92	0.03-0.06	0.036

*Yield based on propellant quantity at time of impact.

In the Seven Chart Approach, the complex question of explosion yield prediction was divided into three parts which were examined separately and independently and then combined to give the desired results. These parts are discussed in the following paragraphs.

C.3.1 The Yield Potential

The yield potential is defined as the maximum theoretical explosive yield which can be produced at any time t if the propellants present are mixed in the most favorable manner. This function can be calculated for any given propellants and selected oxidizer-to-fuel ratio as a function of time using chemical kinetics, heat transfer theory, knowledge of the failure mode and the original configuration of the propellant containers.

C.3.2 Mixing Function

The mixing function is defined as the fraction of the propellants which is actually mixed at any time t. It is only this mixed portion of the propellants which takes part in an explosive yield. The fraction can be defined in terms of volume modified by factors which define the degree of mixing which has taken place, or in terms of contact area between the propellants and/or other like considerations. The mixing function is controlled by the type of propellants, the container size and configuration, and the failure mode. The mixing function always increases from zero at the time of failure to a maximum and then decreases again if ignition does not occur. The mixing function multiplied by the yield function gives the expected yield as a function of time for the propellants, configuration, and failure mode under consideration.

C.3.3 Ignition Time

The ignition time determines what the predicted explosive yield will be since it defines the specific point on the expected yield versus time curves generated. Early ignition results in low yields as does very late ignition. Somewhere between, optimum conditions occur which will produce the maximum explosive yield prediction for the conditions being considered. In the case of the actual

vehicle failures which involve large quantities of propellants, there is the possibility of having early ignition, since many ignition sources would exist, e.g., electrostatic charges, failures of electrical systems, failure of structural members, hot engine parts, etc., which would result in low explosive yields.

C.3.4   Conclusions

It is obvious that the calculation of the yield potential is a complex exercise. Similarly, arriving at the mixing function is equally as difficult. Laboratory experiments have been conducted which were aimed at verifying necessary assumptions. Pellets have been vibration-mixed, wax casts have been made of the mixing process, high speed photographic records have been made of the mixing process, and high sensitivity thermocouple grid records during the mixing period (up to destruct by the explosion) have been analyzed. It is suggested by Dr. Farber that when experimental explosion results are not available or feasible to obtain, the Seven Chart Approach will provide a prediction technique which takes into account the kinds of propellants, vehicle configuration, and failure mode. While the experiments tend to support the theory, not enough data are available yet from use of the actual propellants in simulated scale configuration or in sufficiently large quantities to be conclusive.

C.4   CRITICAL MASS PHENOMENA

The Seven Chart Approach indicates that the explosive yield is a function of the ignition time, which is that period from the start of mixing until ignition occurs. Dr. Farber and his associates were impressed that early ignition occurred frequently with large liquid propellant quantities. Although many sources of ignition are available during a vehicle failure, they considered the possibility that the mixing processes themselves produced ignition as the result of electrostatic charges generated and discharged across vapor bubbles. Laboratory tests have been conducted confirming in fact that an electrical field is generated during the mixing process. Calculations have indicated that a critical mass of about 2300 lb of LO_2/LH_2 would produce a sufficiently strong

charge capable of sparking, thereby causing ignition to occur. These calculations presumed that the mixing was due primarily to boiling of the propellants. If the propellants were brought together more violently, more propellants could be mixed before the voltage build-up occurred. Similarly, if the propellants were mixed more gently, greater quantities could be mixed. It is expected that additional work on the theory of critical mass will be forthcoming in the near future.

APPENDIX C REFERENCES

C-1   E. A. Farber, "Prediction of Explosive Yield and Other Characteristics of Liquid Propellant Rocket Explosions," University of Florida (31 October 1968).

C-2   E. A. Farber, "A Mathematical Model for Defining Explosive Yield and Mixing Probabilities of Liquid Propellants," University of Florida Technical Paper No. 346 (March 1966).

C-3   E. A. Farber, "Explosive Yield Estimates for Liquid Propellant Rockets Based upon a Mathematical Model," University of Florida Technical Paper No. 415A (July 1   ).

C-4   E. A. Farber, "Prediction of Explosive Yield and Other Characteristics of Liquid Propellant Rocket Explosions," University of Florida Technical Paper No. 448 (November 1969).

C-5   E. A. Farber, "A Systematic Approach for the Analytical Analysis and Prediction of the Yield from Liquid Propellant Explosions," University of Florida Technical Paper No. 347 (March 1966).

C-6   "Summary Report on a Study of the Blast Effect of the Saturn Vehicle," Arthur D. Little, Inc. (15 February 1962).

APPENDIX D

Statistical Analysis of Explosive Yield of the Space Shuttle Vehicle if Tank Rupture Occurs on Pad

CONTENTS

TABLES

FIGURES

D.1   GENERAL

The current configuration of the space shuttle in fully loaded condition on the pad contains approximately 4 million lb of LH_2 and LO_2 propellants. Of these, 2.9 million lb of LO_2 and 0.5 million lb of LH_2 are stored in two tanks aboard the booster. The orbiter has two LO_2 tanks with a capacity of 0.25 million lb each and a single LH_2 tank with 0.1 million lb capacity.

The current criteria specify that the TNT equivalence for LO_2-LH_2 propellant combinations is 60%. Based on this equivalency, the facilities siting for the space shuttle would have to be based on a total yield equivalent to 2.4 million lb of TNT.

Studies for other vehicles have indicated that the probability of a failure occurring, such as tank rupture, which could result in the explosion of propellants such as LH_2 and LO_2, is very low. For instance, data from an analysis for the Titan IIIM vehicle indicated that the probability of a tank rupture during the time period from T-30 to T-0 minutes was approximately 0.4×10^{-6}. A specific failure mode and effects analysis has not been made for the space shuttle vehicle; however, it is generally considered that the probability of a tank rupture while on the pad would also be very low.

In spite of the anticipated low probability of a situation occurring which could result in an explosion on the pad, there is the question of the magnitude of the explosion if such an event occurs. This appendix presents a statistical development of the yield of exploding propellants for a multi-tank vehicle configuration such as is used on the space shuttle.

In that analysis, a probability density function for the yield of an explosion was first developed. The properties of that probability density function were then used to establish a probability density function considering the fact that various combinations of tanks of the space shuttle (hence, different quantities of propellants) may be involved in the explosion. The composite probability

density function then was used as the basis for probability statements relative to the yield of the space shuttle propellants.

D.2   APPROACH

In the event of an explosion, the yield, y, may vary from zero to some maximum value, y_n. Many factors obviously affect the yield of the explosion, including the mixing of the propellants. However, adequate information was not available in this study from which to base the development of a probability density function for yield. Therefore, several assumed probability density functions were evaluated in this analysis to show the sensitivity of the results to this input. The various density functions used are discussed in subsequent sections of this appendix.

A basic requirement for each of the probability density functions evaluated was that the following mathematical condition be satisfied:

$$\int_0^1 F(z)dz = 1$$

where f(z) is the probability density function whose value must be equal to or greater than zero for all admissible values of z and $z = 7/y_n$.

Using the assumed distributions on yield, a composite probability density function was then developed as discussed below.

The STS vehicle contains five tanks for which there are 31 possible combinations which may be involved in an explosion. To establish the probability density function for the complete system of tanks, the following ground rules were used:

a.   When the ruptured tank(s) is an O_2 tank, it was assumed that an explosion will not occur but that a fire may result. Subsequent explosions of the other propellants aboard the vehicle as a result of the fire will be low order and will not be considered.

D-2

b. In order to have an explosion involving all the propellants of two or more tanks (one or more of which must contain LH2), the ruptures of the individual tanks have to occur essentially simultaneously to result in a high order explosion rather than a fire.

c. A rupture of a tank induced by impact of debris resulting from the rupture or explosion of another tank would result in fire or subsequent lower order explosions than those associated with the initial rupture and therefore need not be considered

The above assumptions result in a widely varying range of quantities of propellant which may be involved in the explosion. The various combinations of tanks are shown in Table D-1 together with the amount of propellant in each tank and the total propellants that would be involved in each case.

Since there are five tanks in the booster and orbiter, the probability that each of the possible combinations of tanks shown in Table D-1 will be involved in the event must be considered in establishing a probability density function for the complete system of five tanks. Using the above ground rules and the assumption that the tanks are equally likely to fail, the conditional probability that a specific tank will be involved at the time of the rupture is 0.2. The probability that any two specific tanks would be involved was assumed to be $(0.2)(0.2) = 0.04$, etc. Probability values so obtained were then used with the data in Table D-1 and the previously discussed distribution functions to establish the composite probability density function for the complete system.

The equation for the composite probability density function is

$$F(\overline{y}) = \frac{\sum\limits_{n}[P_n F_n(y)]}{\sum\limits_{n} P_n}$$

where

P_n = the probability that tank combination n (as defined in Table D-1) is involved in the initial explosion.

$F_n(y)$ = the density function for tank combination n.

Table D-1. Propellant Tank Combinations and Capacities ($lb \times 10^6$)

Tank Combination, n	Booster		Orbiter			Total	Total Propellants Contributing to Explosion, W_n
	O	H	O	O	H	O/H	
1	2.9					2.9	0.0
2		0.5				0.5	0.5
3			0.25			0.25	0.0
4				0.25		0.25	0.0
5					0.1	0.1	0.1
6	2.9	0.5				3.4	3.4
7	2.9		0.25			3.15	0.0
8	2.9			0.25		3.15	0.0
9	2.9				0.1	3.0	3.0
10		0.5	0.25			0.75	0.75
11		0.5		0.25		0.75	0.75
12		0.5			0.1	0.60	0.60
13			0.25	0.25		0.50	0.0
14			0.25		0.1	0.35	0.35
15				0.25	0.1	0.35	0.35
16	2.9	0.5	0.25			3.65	3.65
17	2.9	0.5		0.25		3.65	3.65
18	2.9	0.5			0.1	3.50	3.50
19	2.9		0.25	0.25		3.40	0.0
20	2.9		0.25		0.1	3.25	3.25
21	2.9			0.25	0.1	3.25	3.25
22		0.5	0.25	0.25		1.0	1.0
23		0.5	0.25		0.1	0.85	0.85
24		0.5		0.25	0.1	0.85	0.85
25			0.25	0.25	0.1	0.60	0.60
26	2.9	0.5	0.25	0.25		3.90	3.90
27	2.9	0.5	0.25			3.75	3.75
28	2.9	0.5		0.25	0.1	3.75	3.75
29	2.9		0.25	0.25	0.1	3.50	3.50
30		0.5	0.25	0.25	0.1	1.10	1.10
31	2.9	0.5	0.25	0.25	0.1	4.0	4.0

D-4

D.3　RESULTS

D.3.1　Model 1

As indicated previously, several probability density function models were evaluated in this study. For Model 1, the following criteria were used as the basis for selection of an appropriate density function:

a. The value of 60% TNT equivalency was assumed to be the mean value, $\bar{y}$, of the probability density function. It was also assumed that all yields in the neighborhood of 60% are highly likely on a relative basis.

b. All values of F(z) in the vicinity of zero yield and the maximum value are relatively low in comparison with the value of F(z) in the vicinity of the mode.

c. It was assumed that the maximum value, y_n, would be based on a TNT equivalency of 100%. That is, the explosive effects would never exceed that for a similar amount of TNT.

Using the above conditions as criteria, a Beta function[*] was selected which has the general equation:

$$F(z) = \frac{(\alpha + \beta + 1)!}{\alpha! \; \beta!} \; z^{\alpha}(1 - z)^{\beta}$$

where

z = normalized form of the random variable (yield)

$= y/y_n$

The Beta function describes a family of curves which is dependent upon a choice of α and β. For this analysis, the desired characteristics of the distribution, for the case where the maximum yield is 100% equivalency, were obtained using a value of $\alpha = 5$. Using this value and the relationship for the mean

$$\bar{z} = \frac{\alpha + 1}{\alpha + \beta + 2}$$

---

[*]See Ref. B-1 for a detailed discussion of the Beta function.

the value of $\beta = 3$ was determined. The equation for the distribution function is then

$$F(z) = 504 \ z^5(1 - z)^3$$

A plot of this equation is shown in Figure D-1. This curve indicates that the most likely equivalency (modal value) is 0.625, whereas the mean value was 0.60. It also shows that there is relatively low probability of equivalencies less than 0.2. This density function in terms of yield is given by the equation

$$F(y) = \frac{504}{y_n} \left(\frac{y}{y_n}\right)^5 \left(1 - \frac{y}{y_n}\right)^3$$

The results of the analysis using the density function shown in Figure D-1 are presented in Figure D-2. The unusual shape of this composite density function at low values of yield results from the basic shape of the probability density function for an individual explosion which was assumed and the low values of yield which result from many combinations of the tanks. This figure shows that the most likely value of yield is less than 0.1×10^6 lb while the expected yield is 0.56×10^6 lb. It is also interesting to note that the 95% cumulative probability occurs at 2.3×10^6 lb. In Figure D-3, the probability of exceeding a given specific yield is plotted.

D.3.2   Model 2

In Figure D-4, the second model considered is shown. In this case the mean value of the distribution of 60% was retained but the maximum value was increased to 150% TNT equivalency to acknowledge the possibility of higher yields than were possible with Model 1.

The composite probability density function and the cumulative probability are plotted in Figures D-5 and D-6. They show that the expected value remains
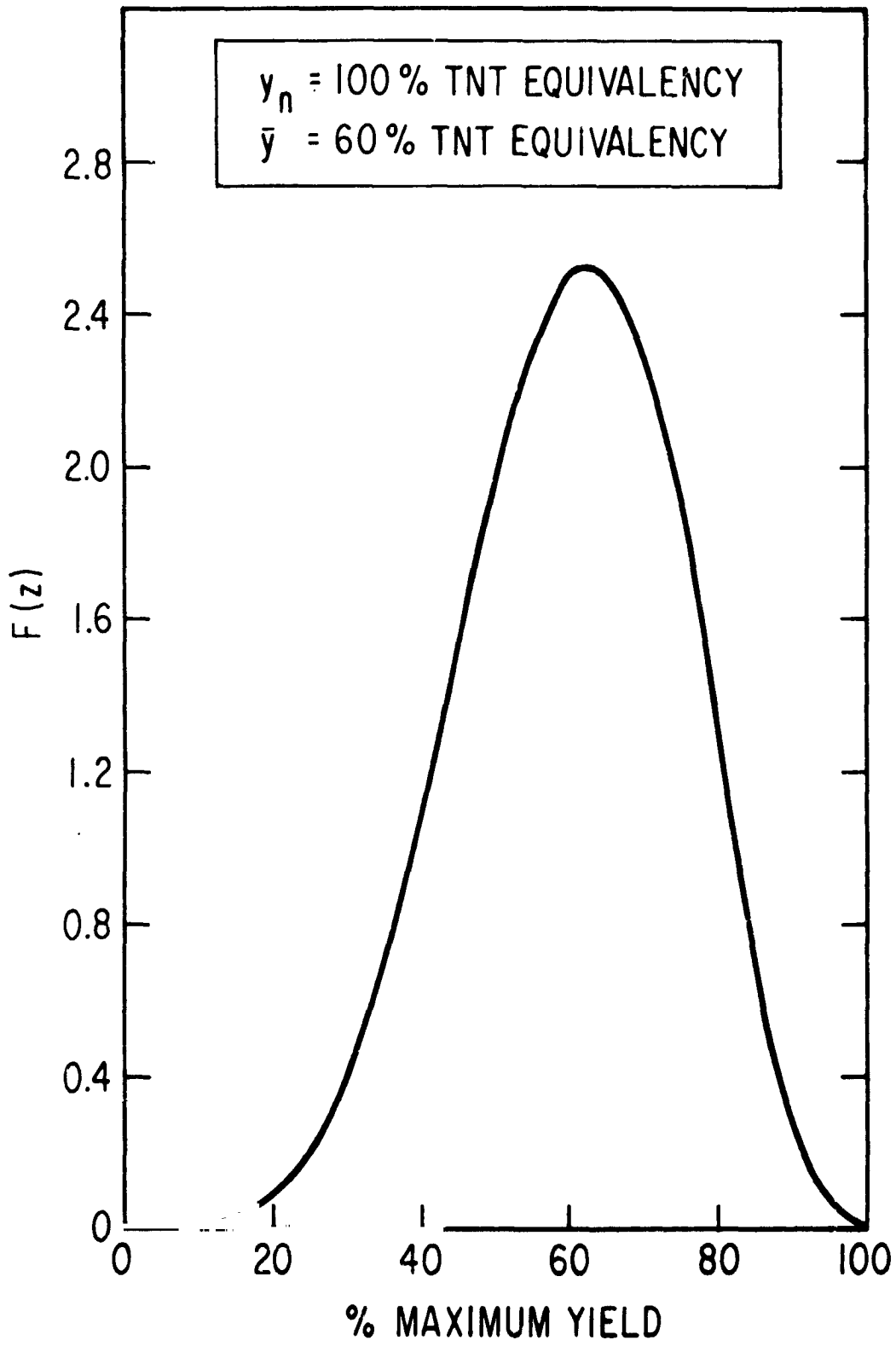
Figure D-1. Probability Density Function - Model 1
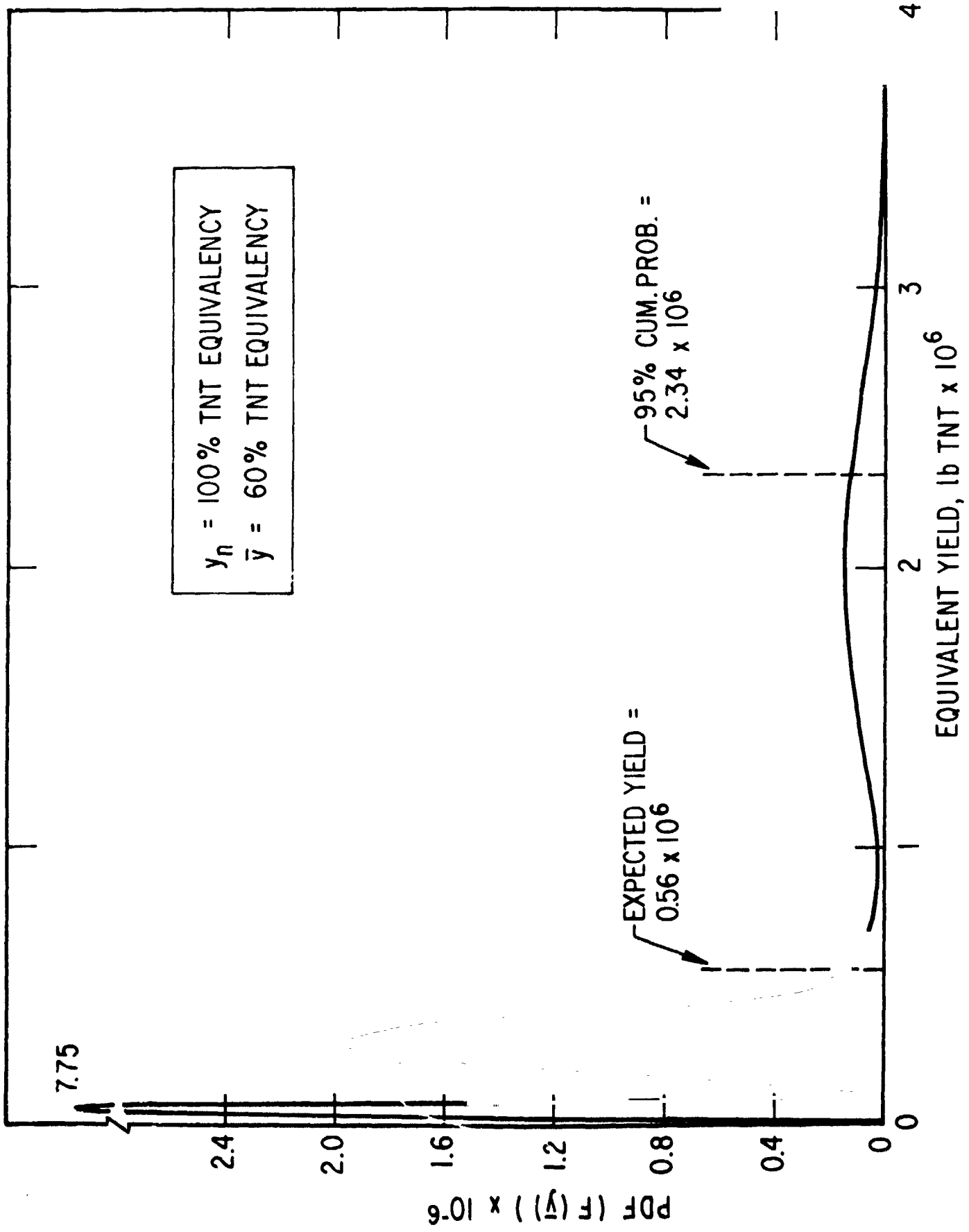
Figure D-2. Composite Probability Density Function – Model 1

The figure axes and labels read:

- Vertical axis (PDF): PDF (F $(\bar{y})$) x 10^{-6} with gridlines at 0, 0.4, 0.8, 1.2, 1.6, 2.0, 2.4, and 7.75
- Horizontal axis: EQUIVALENT YIELD, lb TNT x 10^6 with gridlines at 0, 1, 2, 3, 4

Legend box:
y_n = 100% TNT EQUIVALENCY
$\bar{y}$ = 60% TNT EQUIVALENCY

Annotations:
EXPECTED YIELD = 0.56 x 10^6
95% CUM. PROB. = 2.34 x 10^6

D-8
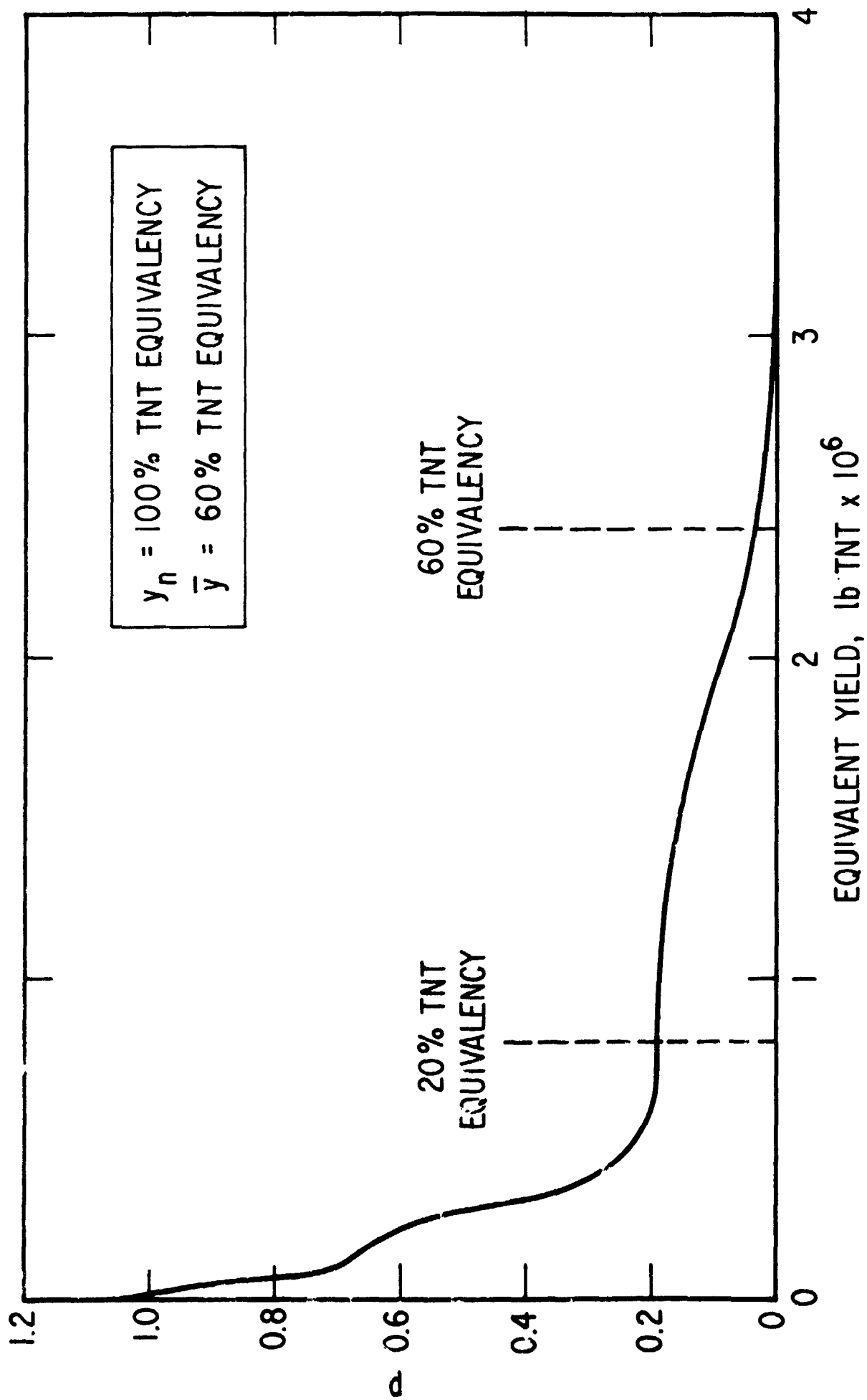
Figure D-3. Probability of Exceeding a Given Yield - Model 1
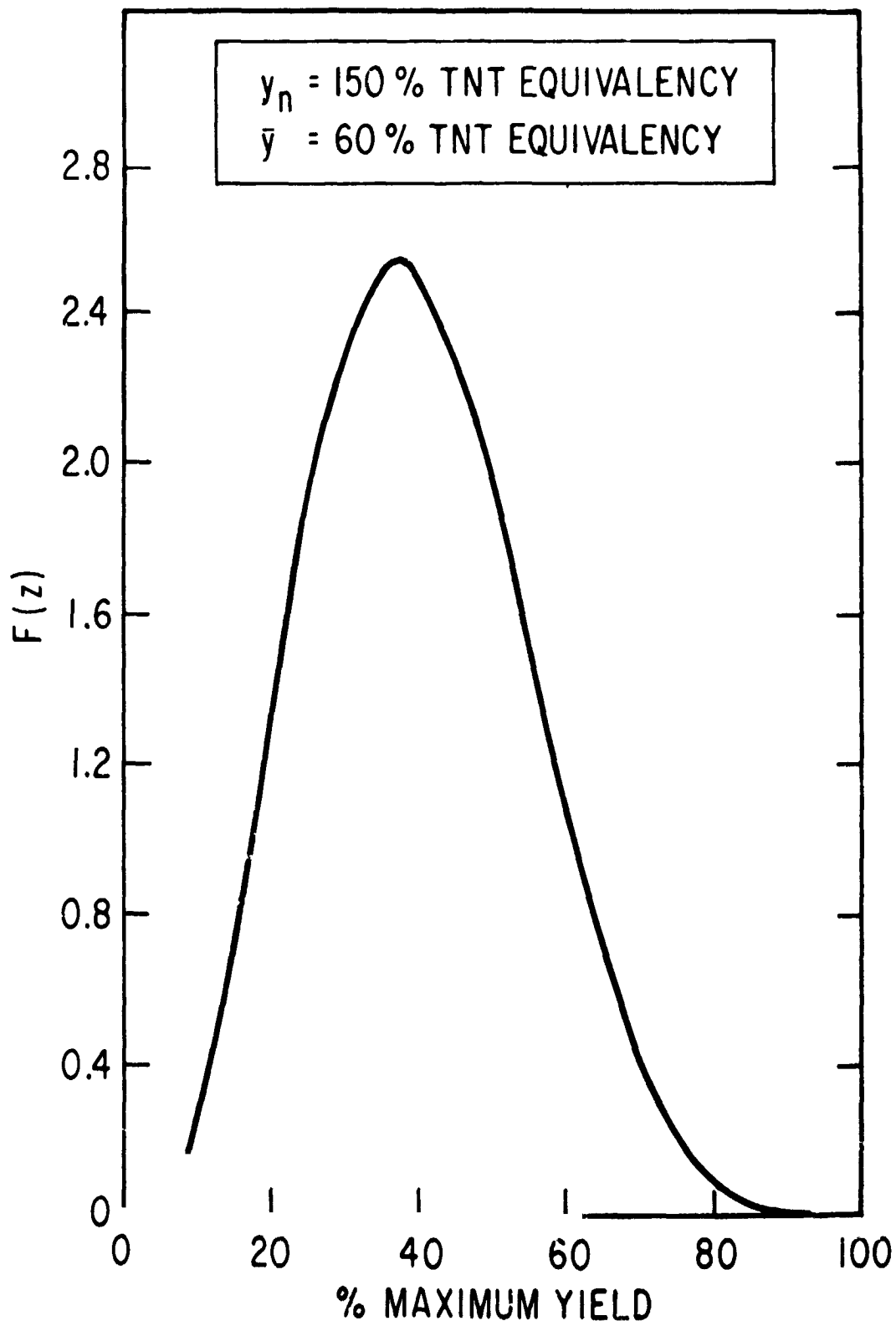
Figure D-4.   Probability Density Function - Model 2
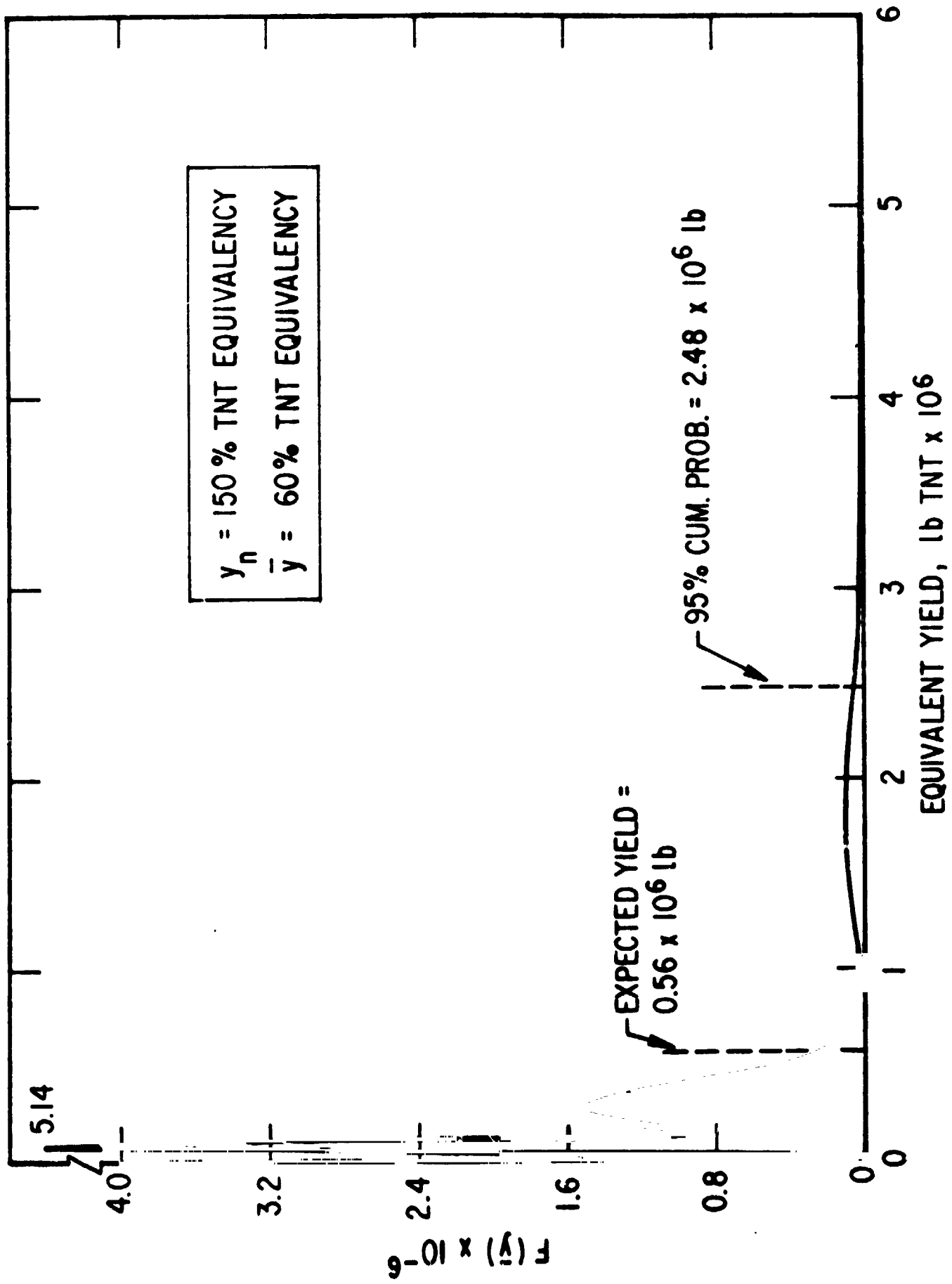
Figure D-5. Composite Probability Density Function – Model 2

Chart labels:
- y_n = 150% TNT EQUIVALENCY
- $\bar{y}$ = 60% TNT EQUIVALENCY
- 95% CUM. PROB. = 2.48×10^6 lb
- EXPECTED YIELD = 0.56×10^6 lb
- EQUIVALENT YIELD, lb TNT $\times 10^6$
- $F(\hat{y}) \times 10^{-6}$
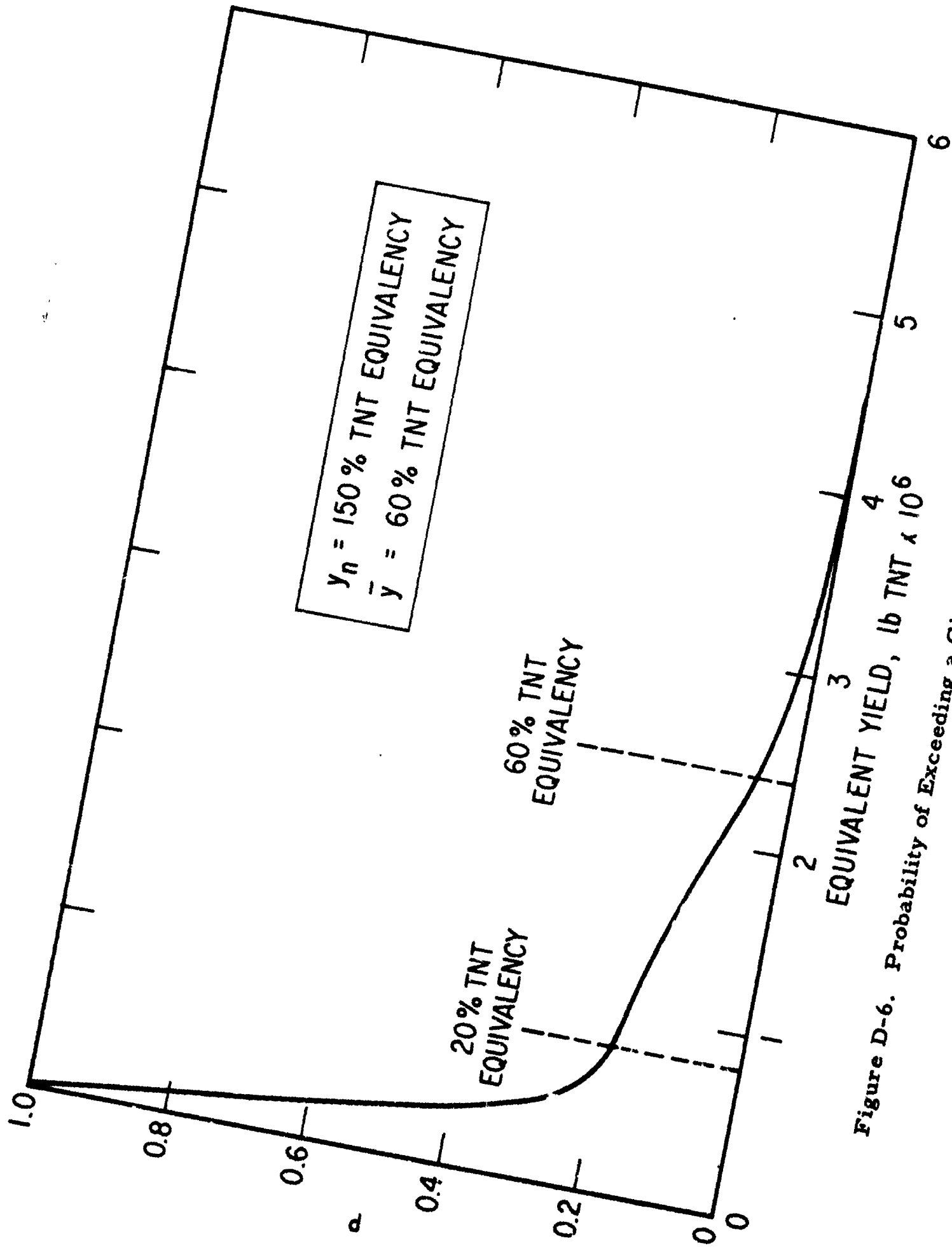
Figure D-6. Probability of Exceeding a Given Yield – Model 2

$y_n = 150\%$ TNT EQUIVALENCY
$\bar{y} = 60\%$ TNT EQUIVALENCY

60% TNT EQUIVALENCY

20% TNT EQUIVALENCY

EQUIVALENT YIELD, lb TNT $\times 10^6$

P

approximately the same as for Model 1 while the 95% cumulative value has increased slightly due to the fact that higher yields are possible using this model.

D. 3. 3   <u>Model 3</u>

In Figure D-7, the probability density function is shown for Model 3. In this model, the mean value of the distribution was assumed to be 20% compared to 60% in the previous analyses. The other general characteristics of the distribution are similar to those in the preceding case.

In Figures D-8 and D-9, the results of the analysis for this model are presented. They show that both the expected value and the 95% cumulative value are reduced substantially from the previous models considered.

D. 3. 4   <u>Model 4</u>

Available experimental data were also used to develop a density function. In Figure D-10, a histogram is presented of TNT equivalencies based on the URS terminal yield data tabulated in Appendix A. The mean value of the TNT equivalencies for these data is 20.4%. It should be noted that these data show that there is a large concentration of very low yields. This contradicts one of the criteria specified for the density function for the previous cases; that is, that values of $F(z)$ in the vicinity of zero yield are relatively low in comparison with values at higher yields. A probability density function was then developed based on these data for use in the analysis.

It should be noted that no effort was made in this portion of the study to verify that these test data actually represent a good statistical sample for application to this type of analysis. For instance, the experimental data were obtained primarily from tests with very small quantities of propellants and the tests were run under conditions which will not exist in the actual vehicle. For this reason, the reader is cautioned against placing any special significance to the results using this model.
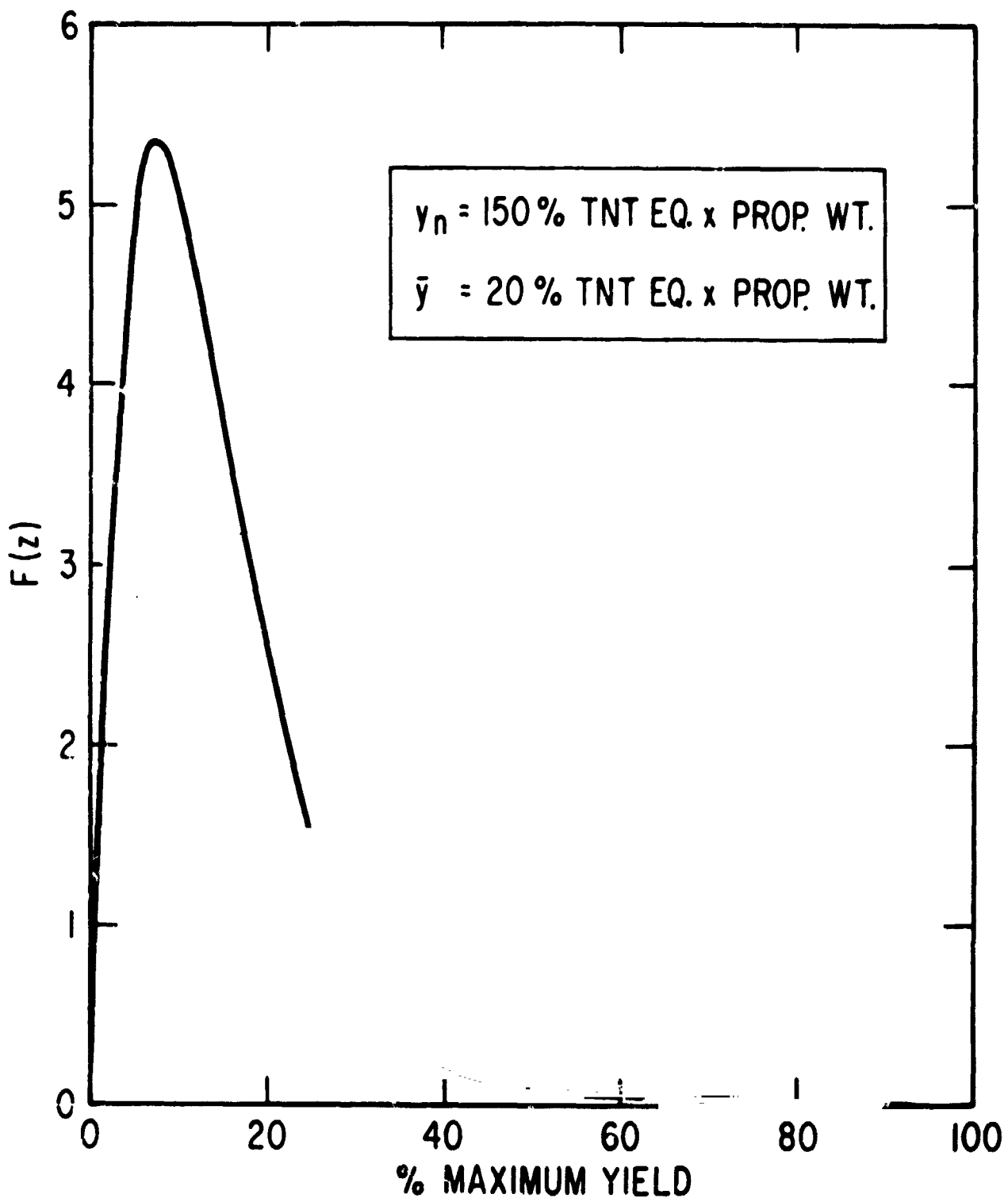
Figure D-7. Probability Density Function - Model 3

The chart contains the following labels and values:

Y-axis: F(z), values 0, 1, 2, 3, 4, 5, 6

X-axis: % MAXIMUM YIELD, values 0, 20, 40, 60, 80, 100

Legend box:
$y_n = 150\%$ TNT EQ. x PROP. WT.
$\bar{y} = 20\%$ TNT EQ. x PROP. WT.
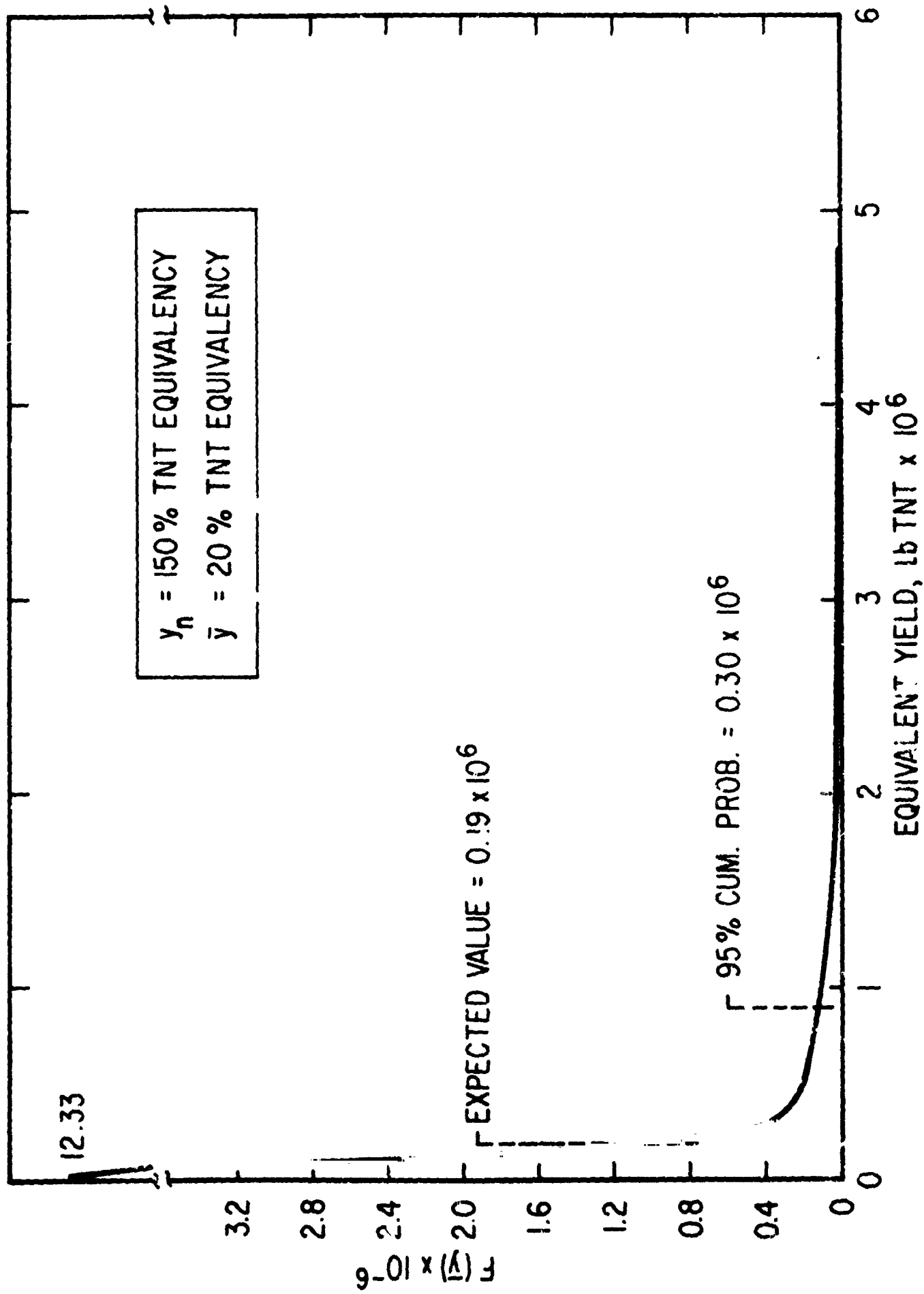
Figure D-8. Composite Probability Density Function – Model 3

Legend on chart:
$y_n = 150\%$ TNT EQUIVALENCY
$\bar{y} = 20\%$ TNT EQUIVALENCY

EXPECTED VALUE $= 0.19 \times 10^6$
95% CUM. PROB. $= 0.30 \times 10^6$

Y-axis: $F(\bar{y}) \times 10^{-6}$
X-axis: EQUIVALENT YIELD, lb TNT $\times 10^6$
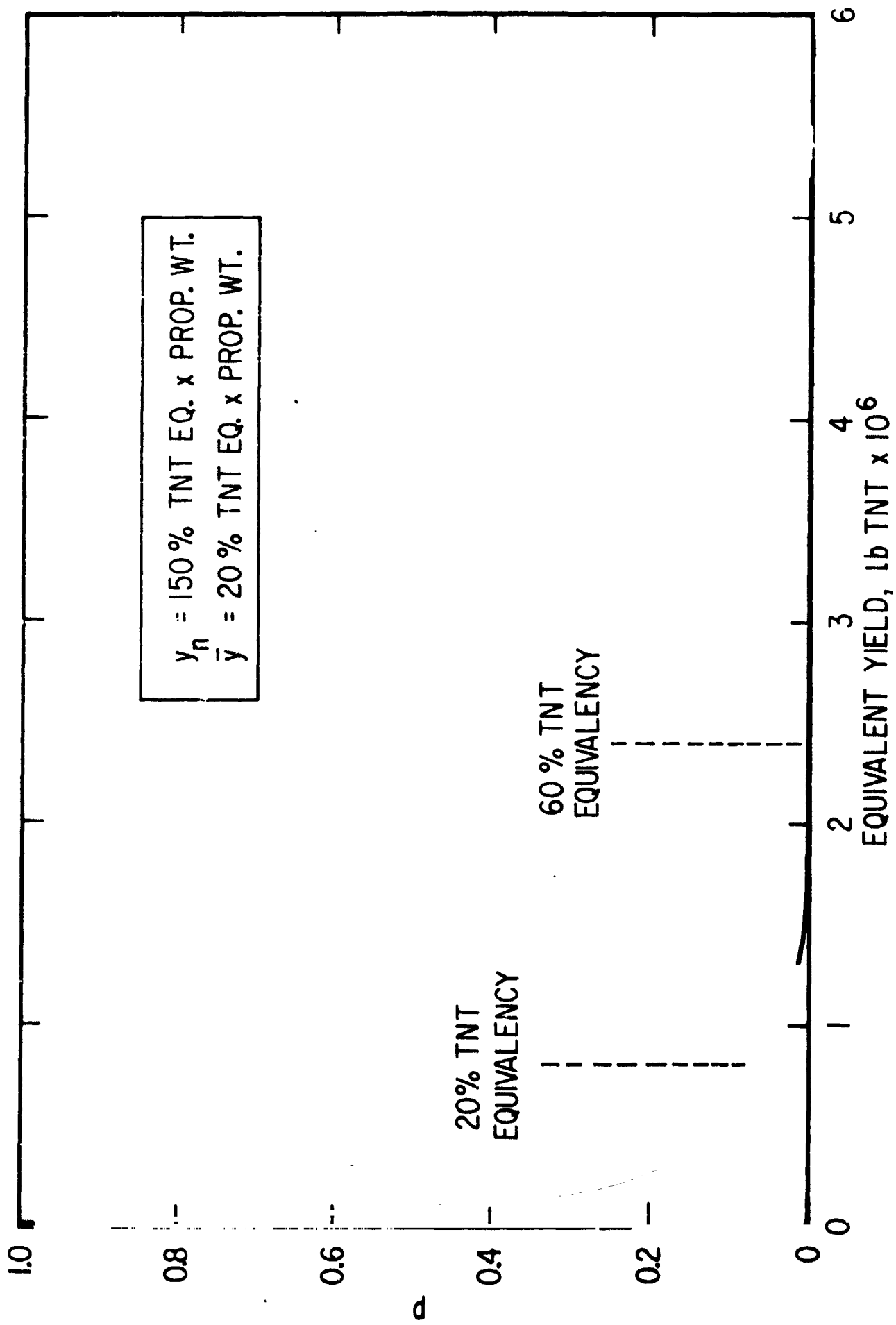
Figure D-9. Probability of Exceeding a Given Yield – Model 3

The plot shows probability p (vertical axis, 0 to 1.0) versus EQUIVALENT YIELD, lb TNT $\times 10^6$ (horizontal axis, 0 to 6).

Legend box:
$y_n = 150\%$ TNT EQ. x PROP. WT.
$\bar{y} = 20\%$ TNT EQ. x PROP. WT.

20% TNT EQUIVALENCY
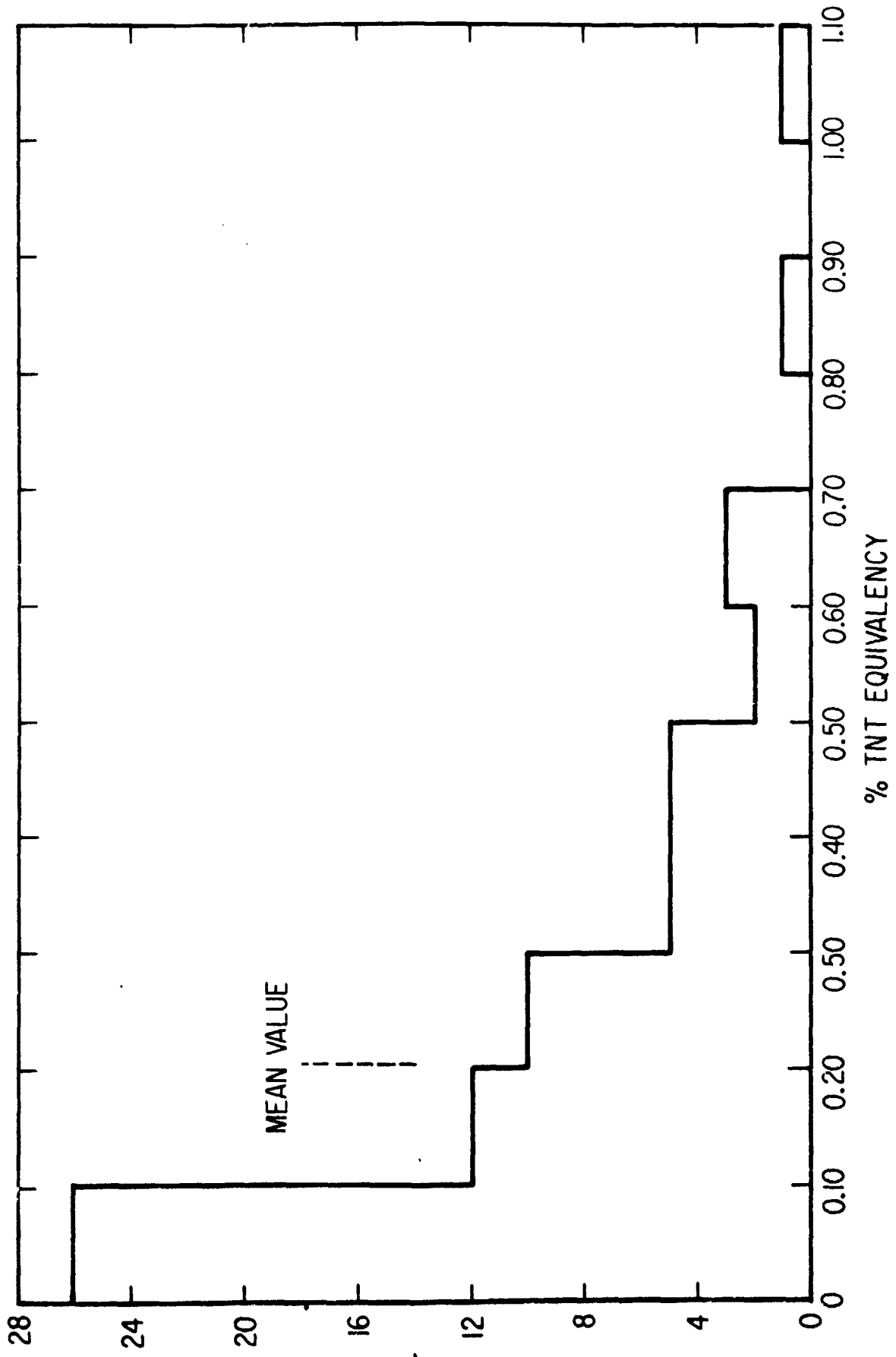
60% TNT EQUIVALENCY

Figure D-10. Histogram-Frequency vs Percent TNT Equivalency
(1968 URS/AFRPL Data)

The Beta function was also used to define the density function for this model. In this case the equation is

$$F(z) = 6.5 (1 - z)^{5.5}$$

The density function defined by this equation has a mean value of 20% as was noted for the experimental data. The density function is plotted in Figure D-11. The correlation between the assumed density function and the experimental data is shown in Figure D-12. In this figure, the horizontal scale is in % TNT equivalency with a maximum value of 150% as was used in Figure D-10 for the experimental data. It should be noted that the $F(z)$ values for the assumed density function are modified in this figure so that the area under the curve remains unity.

In Figures D-13 and D-14, the results of the analysis using the distribution model shown in Figure D-11 are presented. The results of the analysis show that the mean value of yield would be 0.19×10^6 lb, the 95% value would be 0.94×10^6 lb and 0.90×10^6 lb for Model 3 for which the probability density function was assumed without benefit of the test data. However, the mean values of the density functions in both models were the same; i.e., 20%.

The experimental data summarized in Figure D-10 have a mean value of TNT equivalency of approximately 20% and a maximum value of approximately 100%. However, other test data and theoretical studies indicate that even higher equivalencies may occur. Values as high as 300% are considered possible by some sources.

As previously discussed, a maximum value of the TNT equivalency of 100% was first assumed (Model 1). Subsequent calculations (Models 2, 3, 4) were based on a maximum value of 150%. The sensitivity of the Beta distribution function, which was developed based on the experimental data (Model 4), is now summarized for changes in the assumed maximum value of yield. One of the features of the Beta function is that it has, in each case, an upper limit (i.e., it does not admit to values exceeding this limit). The other general characteristics of the Beta distribution function shown in Figure D-11 were retained, including the mean value of 20%.
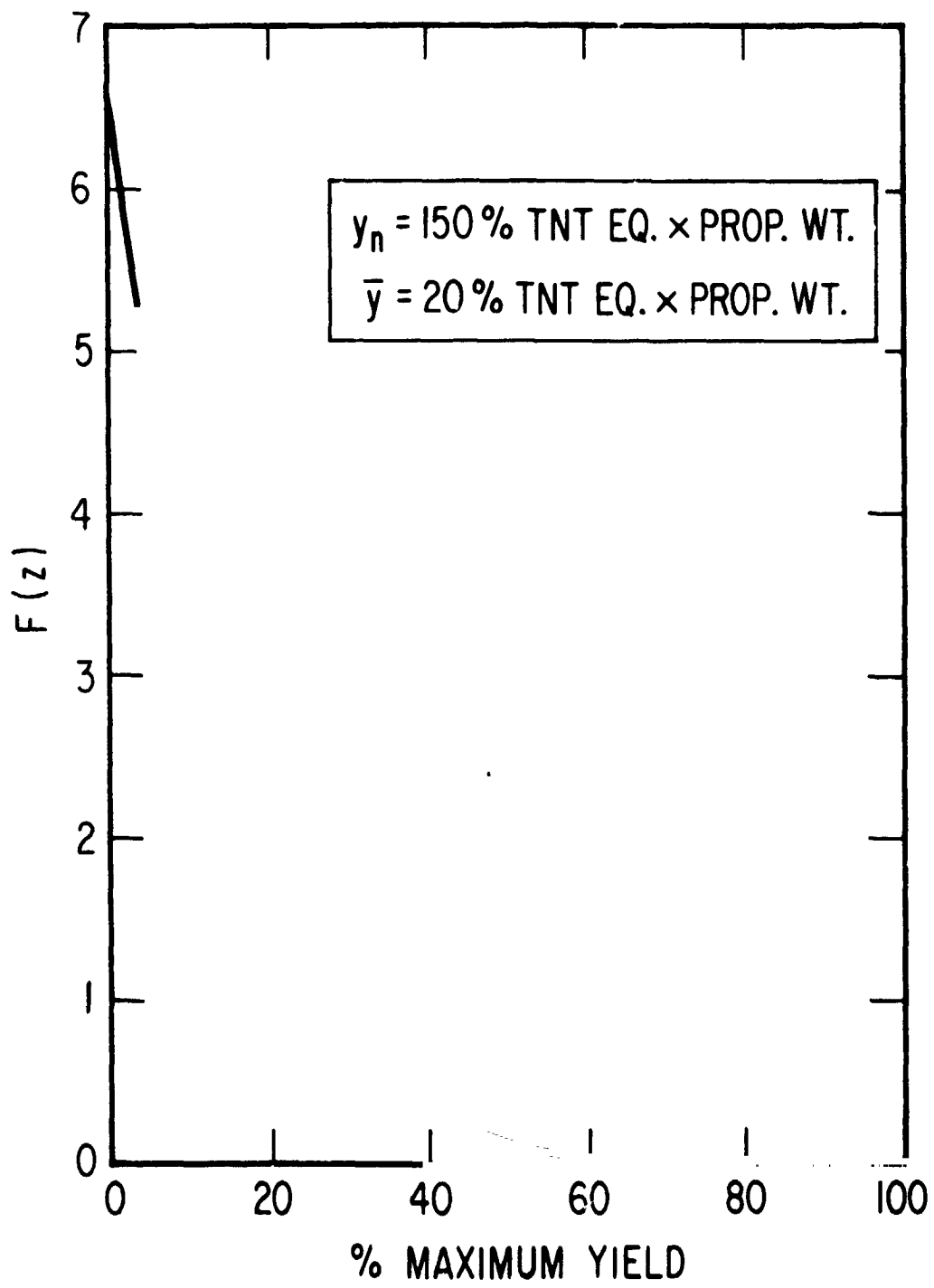
Figure D-11. Probability Density Function - Model 4
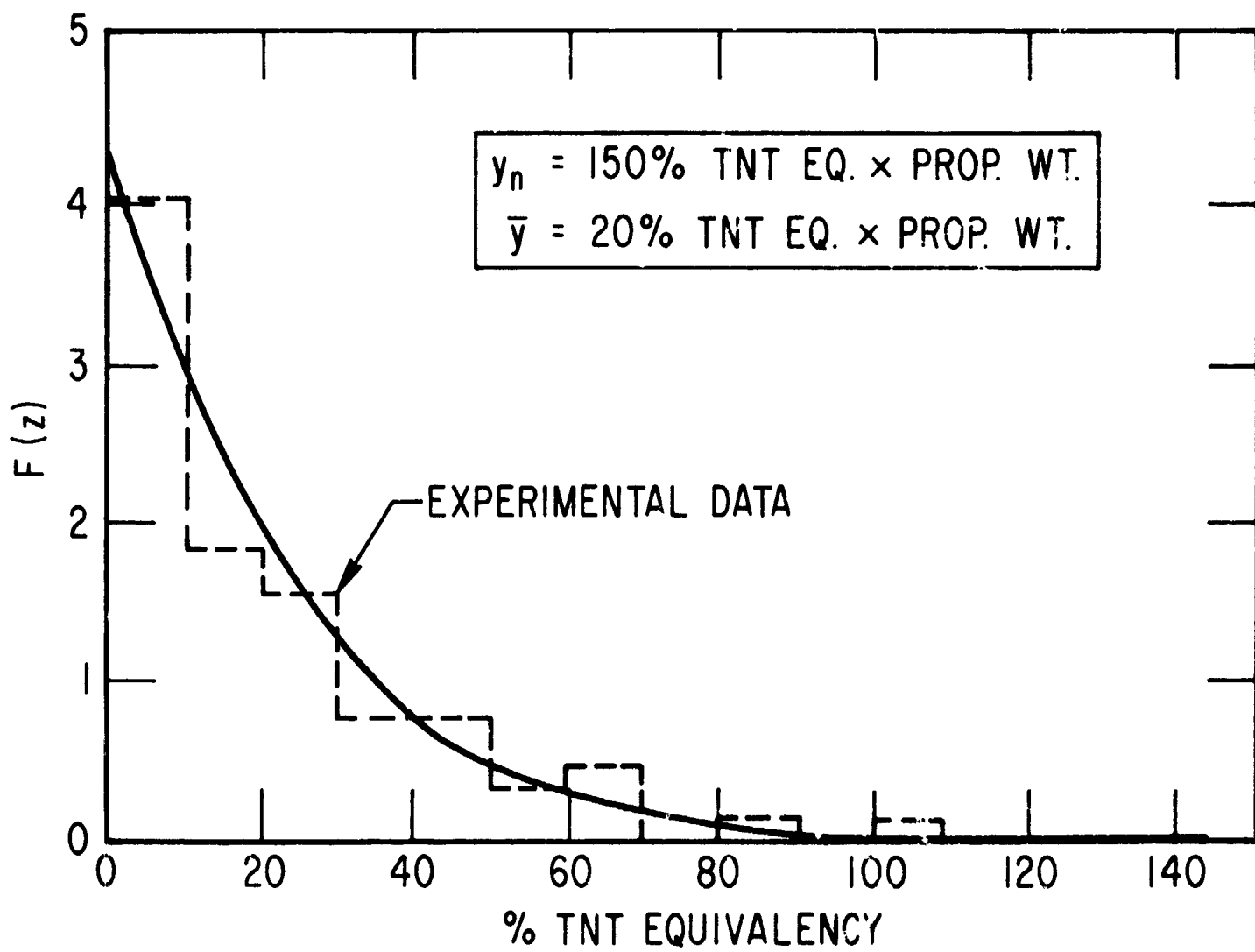
Figure D-12. Comparison of Assumed Probability Density Function, Model 4, to Experimental Data
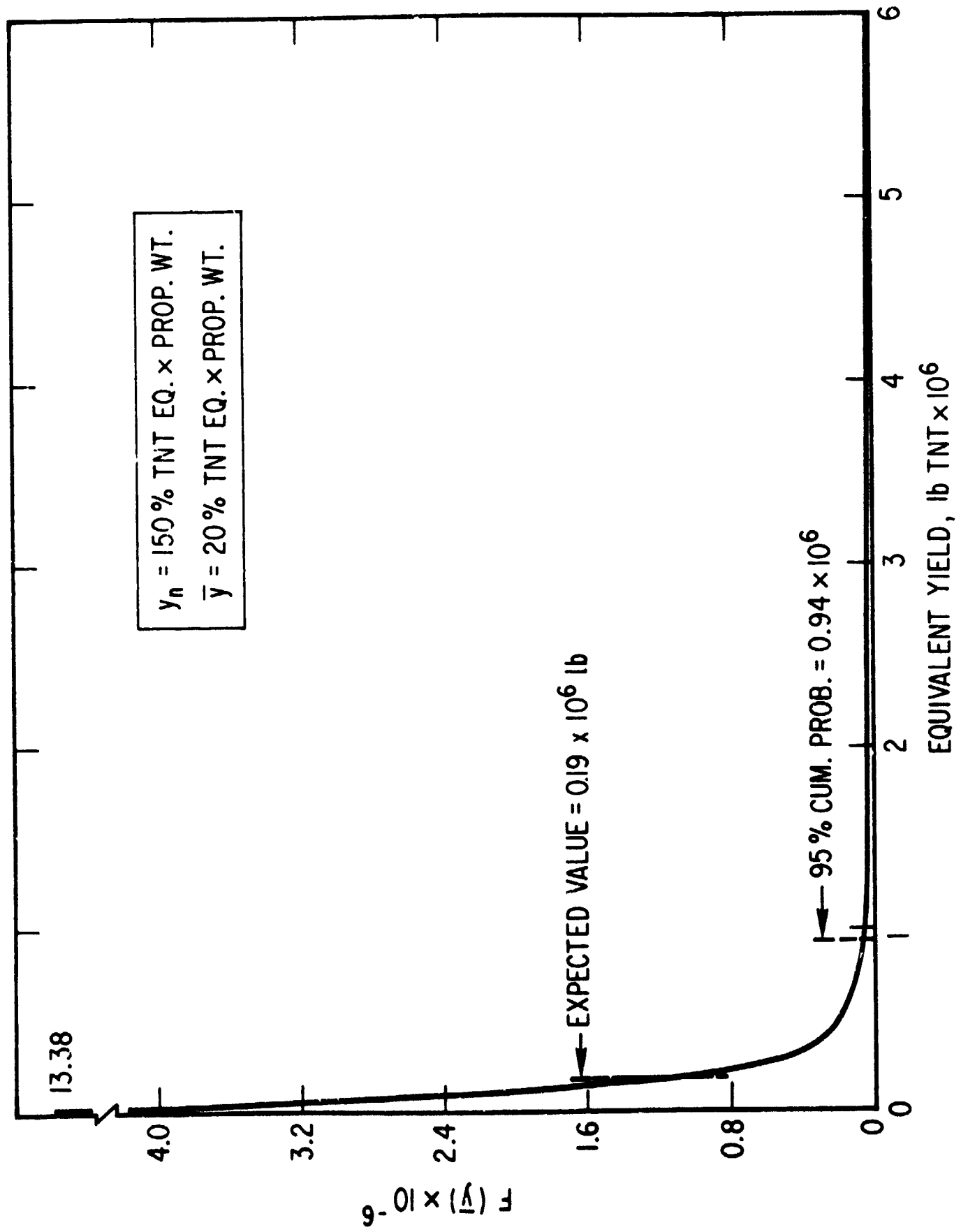
Figure D-13. Composite Probability Density Function – Model 4

The graph shows:
- X-axis: EQUIVALENT YIELD, lb TNT × 10^6
- Y-axis: $F(\bar{y}) \times 10^{-6}$
- $y_n = 150\%$ TNT EQ. × PROP. WT.
- $\bar{y} = 20\%$ TNT EQ. × PROP. WT.
- EXPECTED VALUE = 0.19 × 10^6 lb
- 95% CUM. PROB. = 0.94 × 10^6
- 13.38
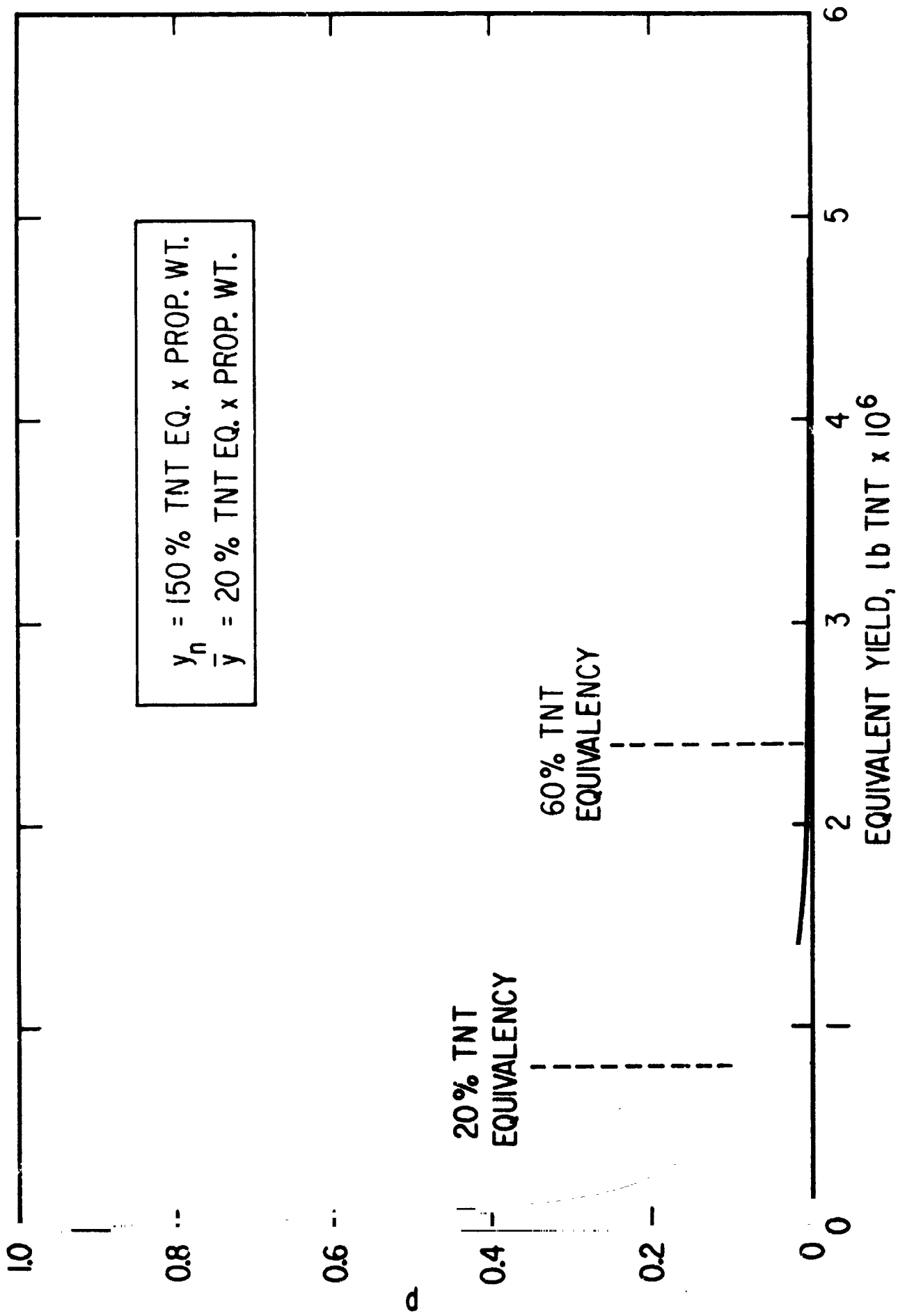
Figure D-14. Probability of Exceeding a Given Yield – Model 4

y_n = 150% TNT EQ. x PROP. WT.
$\bar{y}$ = 20% TNT EQ. x PROP. WT.

60% TNT EQUIVALENCY

20% TNT EQUIVALENCY

EQUIVALENT YIELD, lb TNT x 10^6

p

In Figure D-15, the density function for Model 4 from Figure D-11 (based on 150% maximum TNT equivalency) is shown together with the function for the cases where the maximum value of the distribution is increased to 300% and infinity. As indicated, there is no discernible difference between the 300% case and the infinity case and only minor differences between these cases and the one for a 150% limit. The insignificance of the differences in the data presented in Figure D-15 is further illustrated by comparing the yield/ propellant weight values for certain cumulative values of probability shown below:

Maximum Yield	Yield/Propellant Weight Value for Indicated Cumulative Probability		
	80%	90%	95%
1.5 × Propellant Weight	0.329	0.448	0.554
2.0 × Propellant Weight	0.328	0.451	0.566
2.5 × Propellant Weight	0.327	0.454	0.574
3.0 × Propellant Weight	0.326	0.455	0.578
∞	0.322	0.461	0.599

The above data indicate that the yield/propellant weight value corresponding to a 95% cumulative probability changes approximately 4% when the maximum value (y_n) is doubled and increases approximately 8% for the infinite upper yield case. Thus it is concluded that when the mean value of the density function is established, the effect of the assumption of larger maximum values of yield will be negligible when a Beta function with the general characteristics shown in Figure D-11 is used.

D.3.5   Model 5

In previous sections, a Beta function was used to define the probability that a specific yield would result in event of an explosion. A basic characteristic of this function as used in the preceding analyses is that the probability of occurrence goes to zero at the maximum yield value.
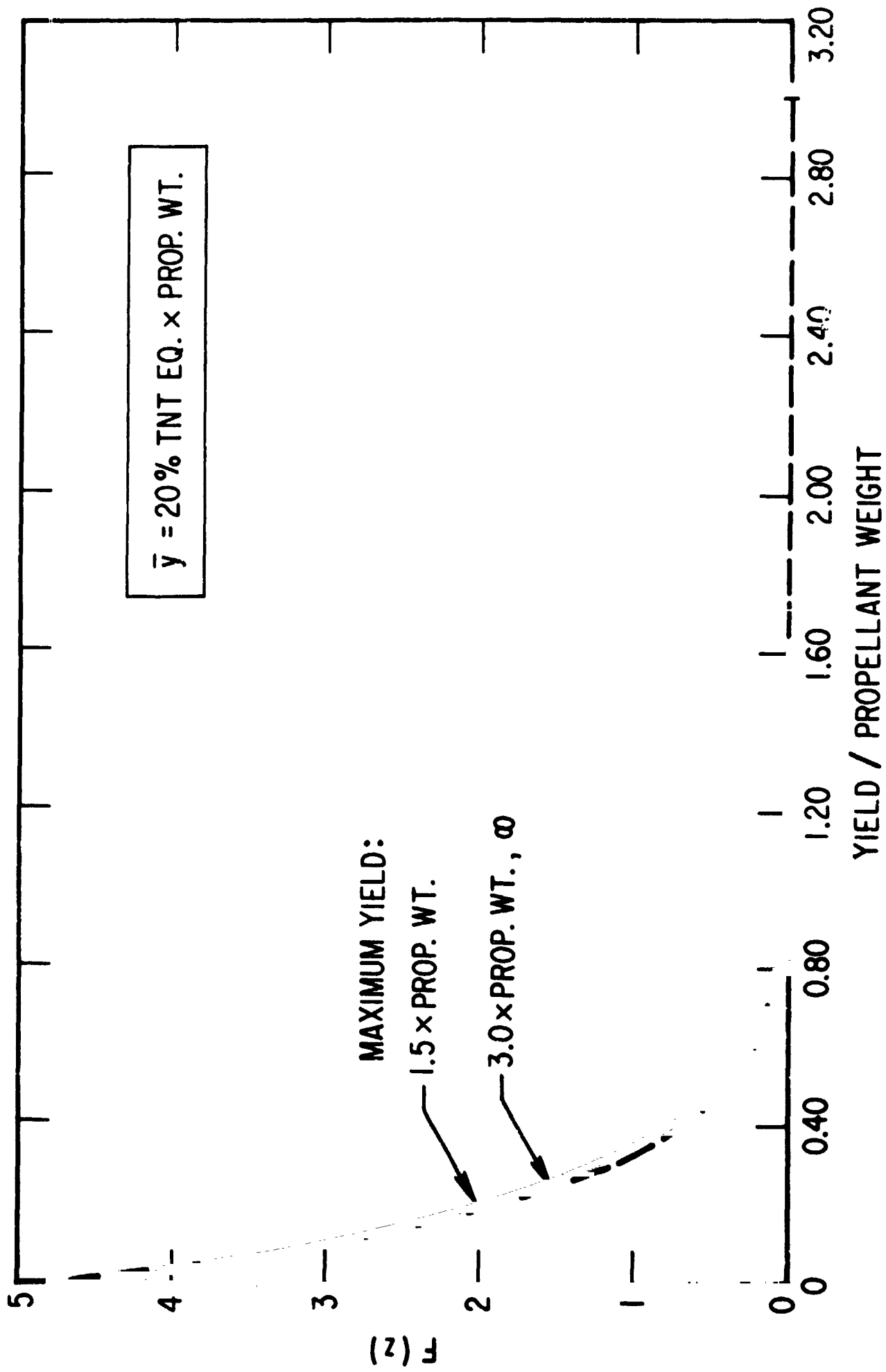
Figure D-15. Comparison of F(z) Values

The question can be asked as to the effect of a distribution which would assume some finite probability that the maximum value will be attained. To evaluate this effect, a uniform distribution of the probability as a function of yield (Figure D-16) was assumed together with a maximum value of 150% TNT equivalency. Under this assumption, there is the same probability (for a given Δz value) that the yield in event of an explosion will be zero, maximum, or some value in between. This distribution is considered very unrealistic when one considers the more or less optimum conditions relative to mixing etc. that must exist to obtain high yields. It is therefore considered as an extreme limit on the range of probability distributions that might be considered. In Figure D-17 the composite probability density function is shown based on this assumed distribution on yield of an explosion and the probability of various amounts of propellant being involved in the explosion. The expected value for this distribution occurs at yield of 0.67×10^6 lb with a 95% cumulative probability occurring at approximately 3.5×10^6 lb.

In Figure D-18, the cumulative probability of the yield exceeding specific values is presented as a function of yield. This figure shows that the probability of exceeding a yield of 1 million lb under this model is 15%. As would be expected because of the characteristics of the distribution assumed, this value is higher than that for the other assumed models.

It should be noted that with the uniform probability model there is approximately one chance in five of exceeding a yield of 0.8×10^6 lb (20% of the 4 million lb of propellants). This value is similar to that for Models 1 and 2 in which a Beta function was used which specifies zero probability that a zero yield or a maximum yield will result. The above comparison shows that the most significant difference is in the probability of attaining high yields. This results from the fact that the uniform distribution acknowledges a significant probability that maximum yields will occur. It should also be kept in mind in reviewing the above results that the uniform distribution model is presented for comparative purposes as a limiting case.
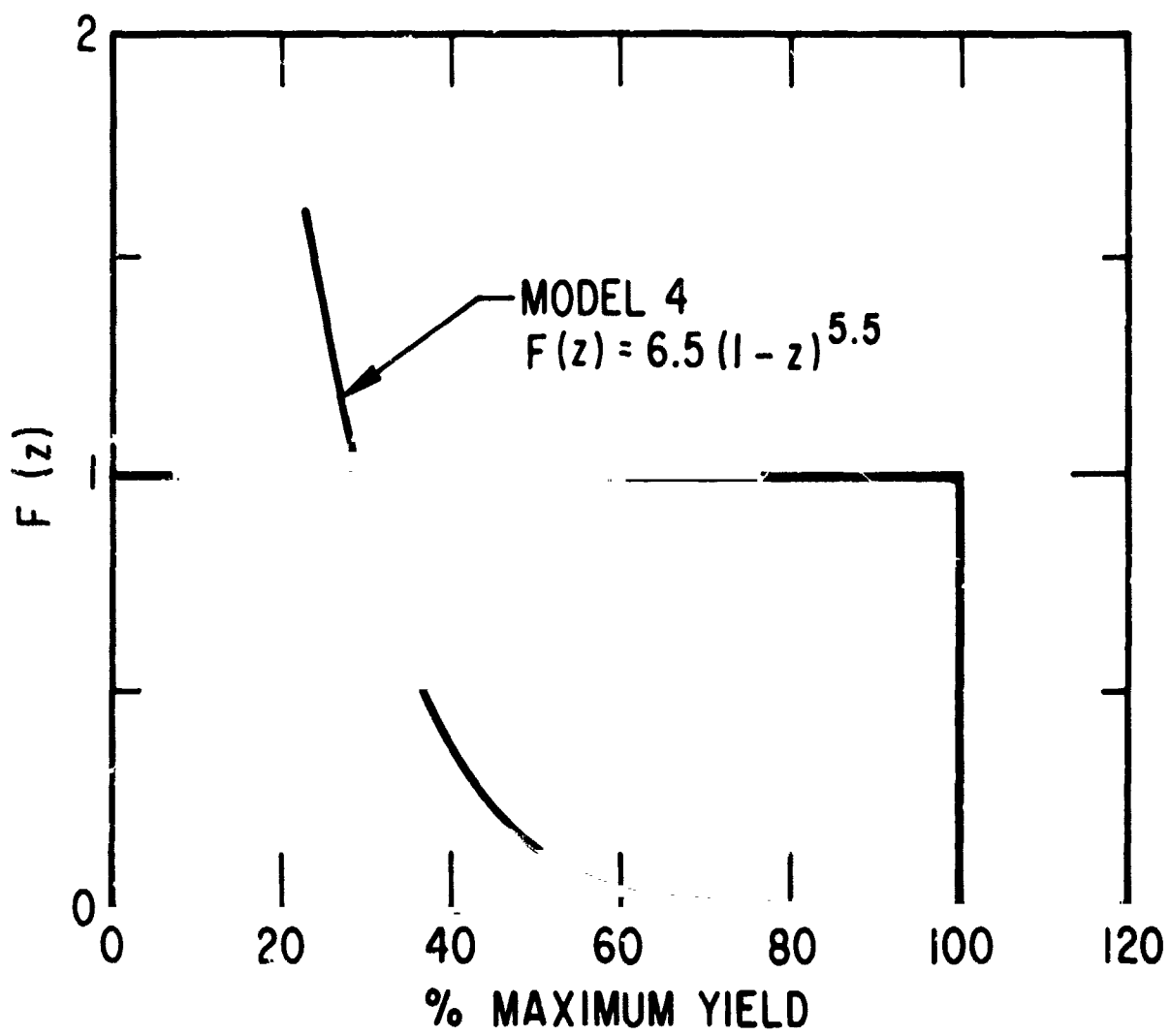
Figure D-16.   Probability Density Function - Model 5
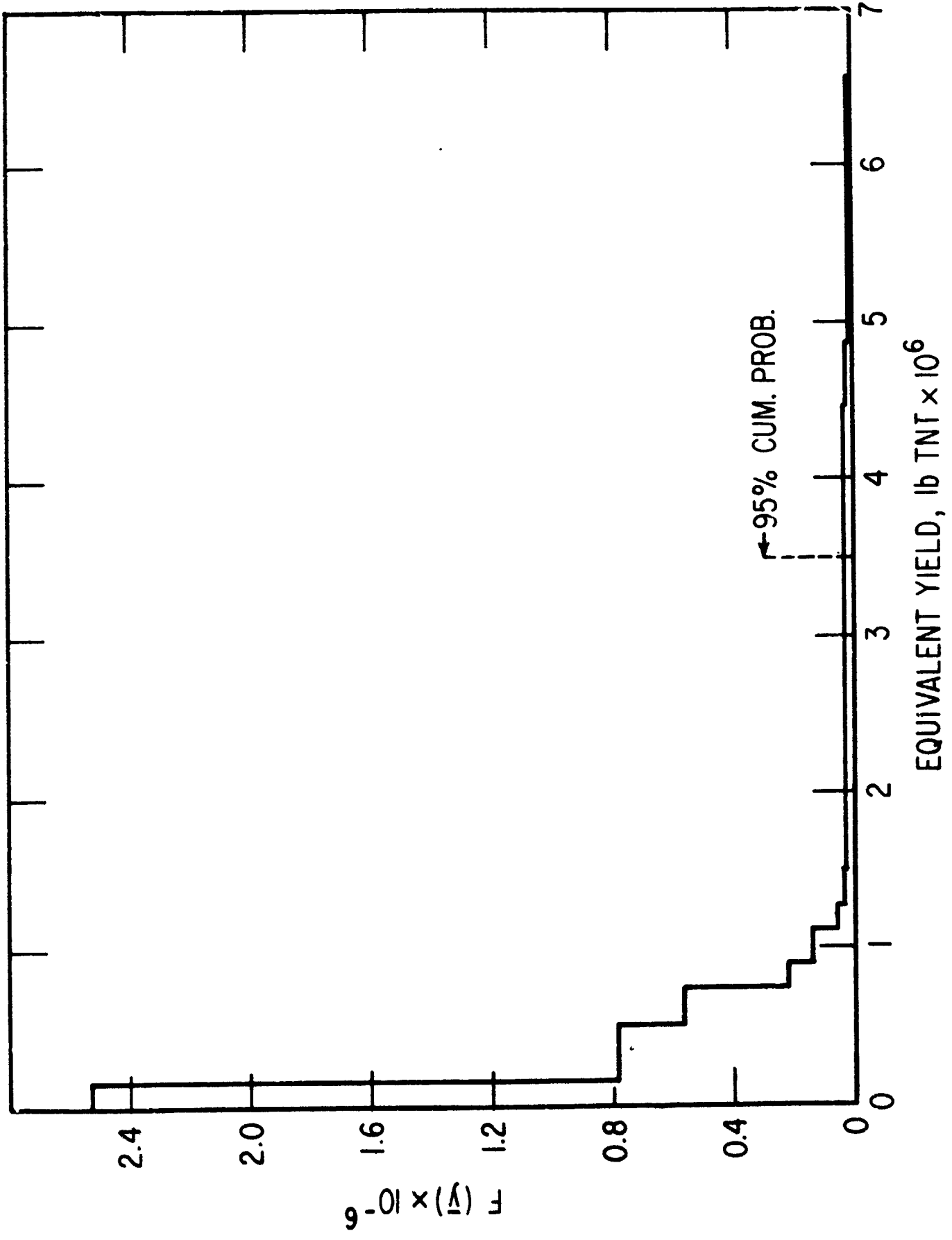
Figure D-17. Composite Probability Density Function – Model 5
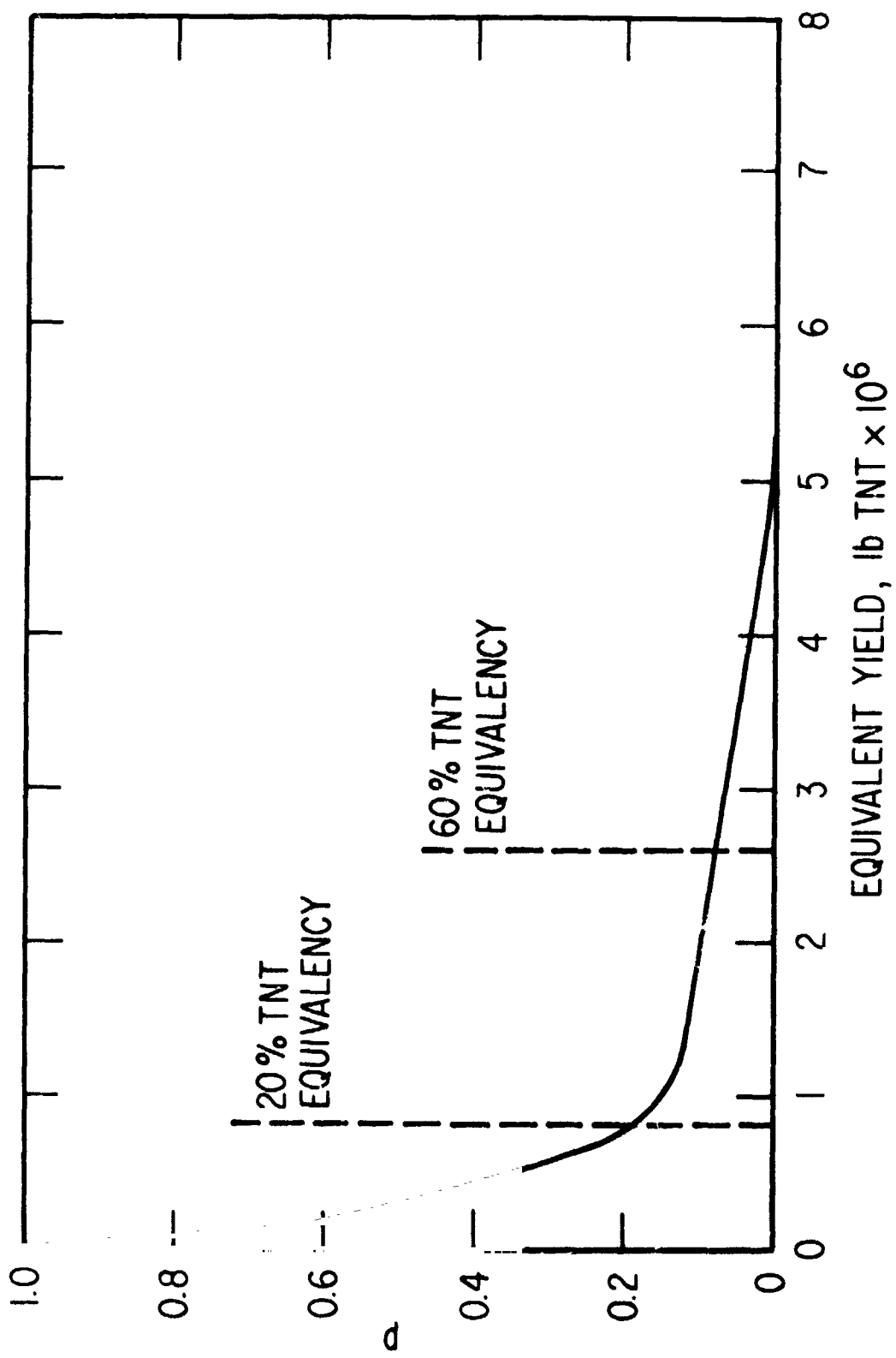
Figure D-18. Probability of Exceeding a Given Yield – Model 5

D. 4   <u>SUMMARY</u>

In Table D-2, the results of the analysis are summarized. It shows that for any of the density functions assumed there is a relatively low probability (conditional) of attaining yields approaching those corresponding to 60% TNT equivalency based on all the propellants aboard the space shuttle. The total probabilities of attaining the indicated yields would be many orders of magnitude less.

It is interesting to note that the lowest probabilities are obtained using Models 3 and 4. Model 3 was based on a Beta function which had zero probability of attaining zero yield or maximum yield and had a mean value of 20%. Model 4 was based on the experimental data which showed a high probability of attaining low yields.

The highest probabilities are generally associated with the uniform distribution. It is emphasized that this is not considered to be a realistic model since it assumes that there is the same probability of attaining any yield including zero and the maximum value.

Table D-2. Comparison of Probability Models Investigated

	Model	Probability of Exceeding		
		0.8×10^6 lb	2.4×10^6 lb	4.0×10^6 lb
1	$y_{max} = 100\%$; $\bar{y} = 60\%$	0.19	0.04	0
2	$y_{max} = 150\%$; $\bar{y} = 60\%$	0.19	0.06	< 0.01
3	$y_{max} = 150\%$; $\bar{y} = 20\%$	0.06	< 0.01	< 0.01
4	(Exp. Data; $y_{max} = 150\%$)	0.06	< 0.01	< 0.01
5	(Uniform Distribution $y_{max} = 150\%$)	0.19	0.09	0.03